

Clusters of Galaxies Overview

- Probes of the history of structure formation
 - Dynamical timescales are not much shorter than the age of the universe
- Studies of their evolution, temperature and luminosity function can place strong constraints on all theories of large scale structure
 - and determine precise values for many of the cosmological parameters

Provide a record of nucleosynthesis in the universe- as opposed to galaxies, clusters probably retain all the enriched material created in them

- Measurement of the elemental abundances and their evolution provide fundamental data for the origin of the elements
- The distribution of the elements in the clusters reveals how the metals were removed from stellar systems into the IGM

Clusters should be "fair" samples of the universe"

- Studies of their mass and their baryon fraction reveal the "gross" properties of the universe as a whole
 - Much of the entropy of the gas is produced by processes other than shocks-
 - a major source of energy in the universe ?
 - a indication of the importance of non-gravitational processes in structure formation ?

Paper for March 5- to volunteers please

Planck intermediate results. X. Physics of the hot gas in the Coma cluster
[2013A&A...554A.140P](#)

Use of the S-Z effect to understand the plasma in the Coma Cluster
(you can gloss over secs 2 & 3 (which are rather technical) and sec 9.4 and 9.5 (which we will not cover in class))

also see

Astrophysics with the Spatially and Spectrally Resolved Sunyaev-Zeldovich Effects. A Millimetre/Submillimetre Probe of the Warm and Hot Universe

Mroczkowski, T.; et al

For the future of this technique, a brief history and lots of technical details- its a bit long (69 pages)

Also our speaker next week M. Gaspari has a relevant paper 2016MNRAS.463..655K Khatri, R, Gaspari, M.

Thermal SZ fluctuations in the ICM: probing turbulence and thermodynamics in Coma cluster with Planck

Today's Material

- How do we know that clusters are massive
 - Virial theorem
 - Lensing
 - X-ray Hydrostatic equilibrium (but first we will discuss x-ray spectra) Equation of hydrostatic equilibrium (*)
- What do x-ray spectra of clusters look like

se Kaiser sec 26.2-26.4

*Hydrostatic equilibrium

$$\nabla P = -\rho_g \nabla \phi(\mathbf{r})$$

where $\phi(\mathbf{r})$ is the gravitational potential of the cluster (which is set by the distribution of matter) P is gas pressure and ρ_g is the gas density ($\nabla f = (\partial f / \partial x_1, \partial f / \partial x_2, \dots, \partial f / \partial x_n)$)

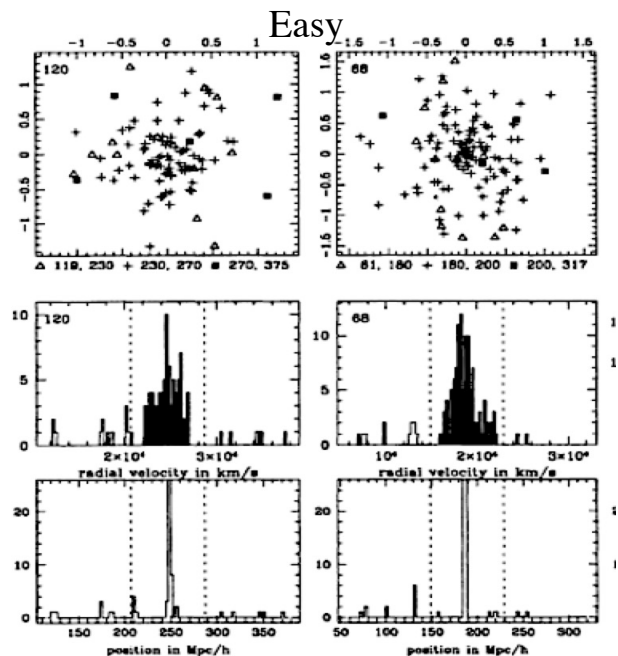
How to Start....Using Galaxy Dynamics

Basic procedure

- first identify the cluster via some sort of signal (e.g. an overdensity of galaxies)
- deduce cluster membership
 - this is not easy and the inclusion of even small fractions of interloper galaxies that are not gravitationally bound to the cluster can lead to a strong mass bias)
- estimate a cluster mass using galaxy positions and velocities as input

Virial theorem

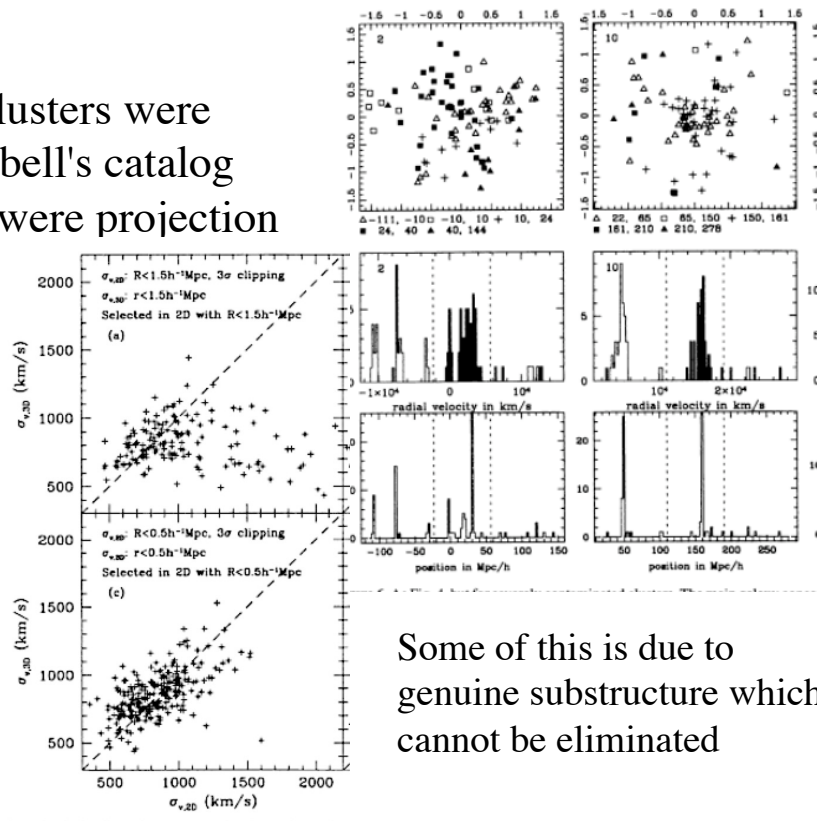
Jeans eq



bottom panel is 'true' distance of clusters, middle is velocity histogram, top is position of galaxies + for galaxies in cluster
van Haarlem, Frenk and White 1997

- Hard- these clusters were included in Abell's catalog because they were projection effects

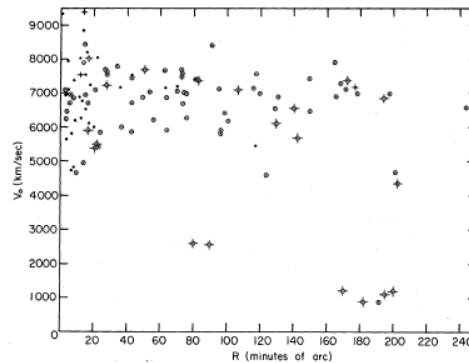
Comparison of observed vs true velocity dispersions for 'tight' vs loose selection criteria



Some of this is due to genuine substructure which cannot be eliminated

The First Detailed Analysis

- Rood et al used the King (1969) analytic models of potentials (developed for globular clusters) and the velocity data and surface density of galaxies to infer a very high mass to light ratio of ~ 230 .
- Since "no" stellar system had $M/L > 12$ **dark matter was necessary**



Rood 1972- velocity vs position of galaxies in Coma

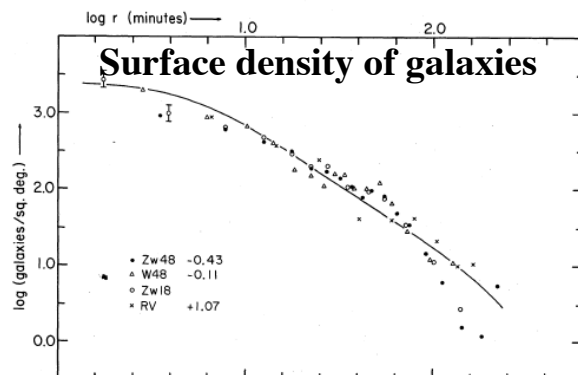


FIG. 5.—Surface densities, corrected for backgrounds given in table 2. For this fitting, logarithms of

Paper is worth reading ApJ 175,627

Virial Theorem (Read Longair 3.5.1; see also Kaiser sec 26.3)

- The virial theorem states that, for a stable, self-gravitating, spherical distribution of equal mass objects (stars, galaxies, etc), the total kinetic energy of the objects is equal to -1/2 times the total gravitational potential energy.

$$U \sim 1/2 GN^2 m^2 / R_{\text{tot}} = 1/2 GM_{\text{tot}}^2 / R_{\text{tot}}$$

(eq 3.13 Longair dimensional analysis)

If the orbits are random
 $KE = 1/2 U$ (virial theorem)
 $M_{\text{tot}} \sim 2Rv_{\text{tot}}^2 / G$

$$2\langle T \rangle = -\langle U_{\text{TOT}} \rangle$$

T is the time average of the Kinetic energy and U is the time average of the potential energy In other words, the potential energy must equal 1/2 the kinetic energy.

No assumptions been made about the orbits or velocity distributions of the particles.

The virial theorem applies to all cases provided the system is in dynamical equilibrium- "virialized"

- Consider a system of N particles with mass m and velocity v.
- kinetic energy of the total system is K.E. (system) = 1/2 m N v² = 1/2 M_{tot} v²

For more detailed derivation see Longair eqs 3.4-3.16

Virial Theorem Actual Use (Kaiser 26.4.2)

- Photometric observations provide the surface brightness Σ_{light} of a cluster. Measurements of the velocity dispersion σ_v^2 together with the virial theorem give $\sigma_v^2 \sim U/M \sim GM/R \sim G\Sigma_{\text{mass}} R$
 Σ_{mass} is the projected mass density.

At a distance **D** the mass to light ratio (M/L) can be estimated as
 $M/L = \Sigma_{\text{mass}} / \Sigma_{\text{light}} = \sigma_v^2 / GD\Theta \Sigma_{\text{light}}$; Σ_{light} is the surface brightness- a direct measurable

Notice all the terms are observable !

where Θ is the angular size of the cluster. (see Kaiser eq 26.13)

- The virial theorem is exact, *but requires that the light traces the mass-it will fail if the dark matter has a different profile from the luminous particles.*

Mass Estimates

- While the virial theorem is fine it depends on knowing the time averaged orbits, the distribution of particles etc etc- a fair amount of systematic errors
- If the system is spherically symmetric, a suitably weighted mean separation R_{cl} can be estimated from the observed surface distribution of stars or galaxies and so the gravitational potential energy can be written $|U| = GM^2/R_{cl}$.
- The mass of the system is using $T = \frac{1}{2} |U|$
- $M = 3\sigma^2 R_{cl}/G$. (The & White 1986); R_{cl} depends on the density distribution
- **In useful units this gives $M=3R_G \sigma_v^2/G= 7.0 \times 10^{12} R_G (\sigma_v)^2 M_\odot$**

where R is in units of Mpc and σ_v is in units of 100km/sec

Would like better techniques

- Gravitational lensing
- Use of spatially resolved x-ray spectra

Mass Estimate

- As pointed out by Longair The application of the theorem to galaxies and clusters is not straightforward.
- only radial velocities can be measured from the Doppler shifts of the spectral lines, not the 'true' velocity dispersion.
- Assumptions need to be made about the spatial and velocity distributions of stars in
- the galaxy or the galaxies in a cluster e.g :that the galaxies have the same spatial and velocity distribution as dark matter particles, and that all galaxies have the same mass
- If the velocity distribution is isotropic, the velocity dispersion is the same in the two perpendicular directions as along the line of sight and so $\langle v^2 \rangle = 3\langle v_r \rangle^2$ where v_r is the radial velocity which is measureable.

If the velocity dispersion is independent of the masses of the stars or galaxies, the total kinetic energy is $T = \frac{3}{2} M \langle v_r \rangle^2$ (3.18)

- If the system is spherically symmetric, a suitably weighted mean separation R_{cl} can be estimated from the observed surface distribution of stars or galaxies and so the gravitational potential energy is

$|U| = GM^2/R_{cl}$ and thus using the virial theorem $M=3\langle v_r \rangle^2 R_{cl}/G$ 3.18 (Longair)

Mass Determination

- for a perfectly spherical system one can write the **Jeans equation for a spherical system** where ν is the density of a tracer - this is used a lot to derive the mass of elliptical galaxies
- Anisotropy parameter $\beta(r) = 1 - \sigma_\theta^2 / \sigma_r^2$

$$GM(\leq r) = -r\sigma_r^2 \left\{ \left[\frac{d \ln \nu}{d \ln r} + \frac{d \ln \sigma_r^2}{d \ln r} \right] + 2\beta(r) \right\}$$

$$\sigma_\phi^2 = \sigma_\theta^2 \quad \text{Spherical symmetry.} \quad \begin{array}{l} \sigma_r^2 \ll \sigma_\theta^2 \quad \text{Nearly circular} \\ \sigma_r^2 \gg \sigma_\theta^2 \quad \text{Nearly radial} \end{array}$$

•Notice the nasty terms

All of these variables are 3-D; we observe projected quantities !

Both rotation and random motions (σ -dispersion) can be important.

Standard practice is to make an a priori assumption about form of potential, density distribution or velocity field.

<https://ned.ipac.caltech.edu/level5/Sept03/Merritt/Merritt2.html>

11

Jeans Equation and Dynamics

- Assumes stationarity, the absence of streaming motions, and spherical symmetry, and is the first velocity moment of the collisionless Boltzmann equation

With no rotation one has the somewhat simpler form

$$\nu GM(r)/r^2 = -d(\nu \sigma_r^2)/dr - (2\nu/r) * (\sigma_r^2 - \sigma_\theta^2)$$

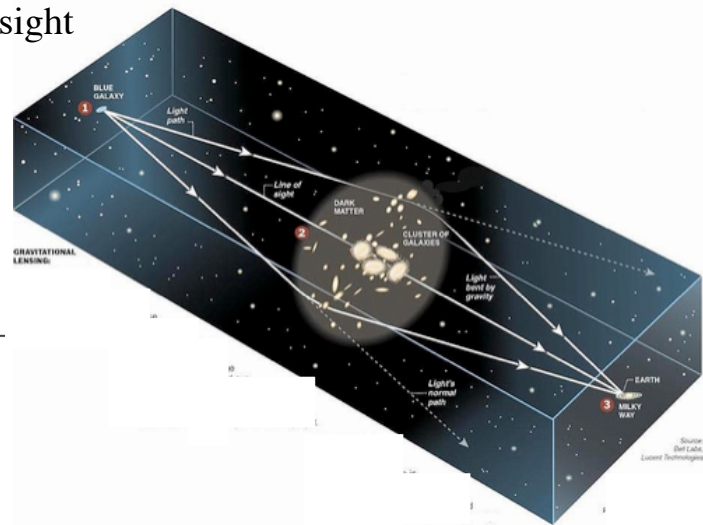
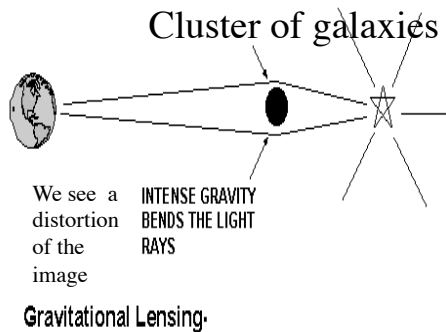
The tracer's velocity anisotropy profile, $\beta(r) = 1 - \sigma_\theta^2 / \sigma_r^2$

$\beta \rightarrow -\infty$ for circular orbits; $\beta = 1$ for radial orbits; $\beta = 0$ for an isotropic velocity field.

- However since the number of unknowns exceeds the number of equations, one needs to make some assumptions to break the degeneracy between the mass and anisotropy profiles - one normally makes assumptions about the form of the potential and the value of β

Light Can Be Bent by Gravity- [Read sec 4.7 Longair](#)
 gravitational lensing. Light rays propagating to us through the inhomogeneous universe are distorted by mass distributed along the line of sight

The 'more' mass- the more the light is bent



faculty.lsmsa.edu

Amount and type of distortion is related to amount and distribution of mass in gravitational lens

Zwicky Again

Zwicky 1937

Nebulae as Gravitational Lenses

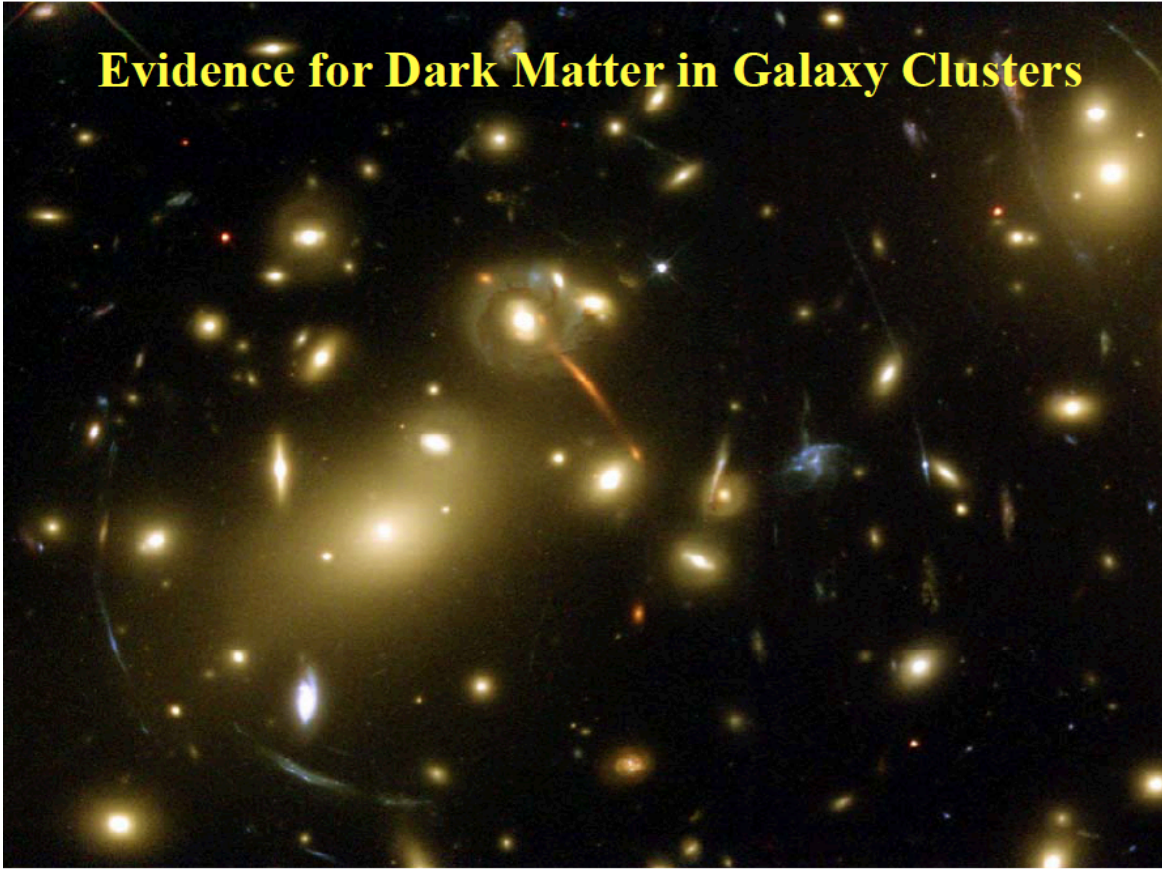
The discovery of images of nebulae which are formed through the gravitational fields of nearby nebulae would be of considerable interest for a number of reasons.

(1) It would furnish an additional test for the general theory of relativity.

(2) It would enable us to see nebulae at distances greater than those ordinarily reached by even the greatest telescopes. Any such *extension* of the known parts of the universe promises to throw very welcome new light on a number of cosmological problems.

(3) The problem of determining nebular masses at present has arrived at a stalemate. The mass of an average nebula until recently was thought to be of the order of $M_N = 10^9 M_\odot$, where M_\odot is the mass of the sun. This estimate is based on certain deductions drawn from data on the intrinsic brightness of nebulae as well as their spectrographic rotations. Some time ago, however, I showed² that a straightforward application of the virial theorem to the great cluster of nebulae in Coma leads to an average nebular mass four hundred times greater than the one mentioned, that is, $M_N' = 4 \times 10^{11} M_\odot$. This result has recently been verified by an investigation of the Virgo cluster.³ Observations on the deflection of light around nebulae may provide the most direct determination of nebular masses and clear up the above-mentioned discrepancy.

Evidence for Dark Matter in Galaxy Clusters

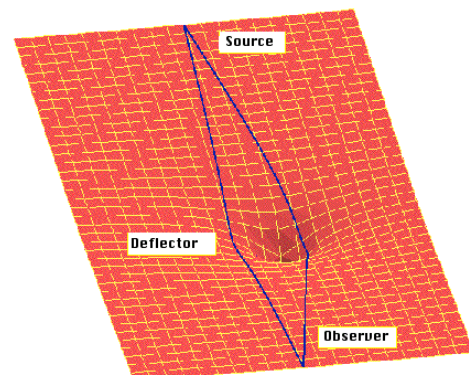
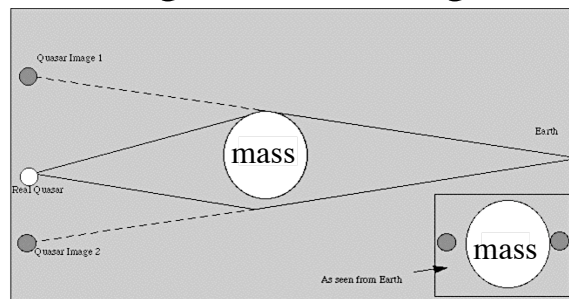


Basics of Gravitational Lensing Sec 4.7 Longair

- See Lectures on Gravitational Lensing by Ramesh Narayan Matthias Bartelmann or <http://www.pgss.mcs.cmu.edu/1997/Volume16/physics/GL/GL-II.html>

For a detailed discussion of the problem

- Rich centrally condensed clusters can produce **giant arcs** when a background galaxy happens to be aligned with one of the cluster caustics*. Can have multiple images
- Every cluster produces **weakly distorted images of large numbers of background galaxies**.
 - These images are called arclets and the phenomenon is referred to as weak lensing.
- The deflection of a light ray that passes a point mass M at *impact parameter* b is eq 4.28



$$\Theta_{\text{def}} = 4GM/c^2b; R_{\text{Sch}} = 2GM/c^2$$

Caustics- see Kaiser 8.1

- Consider a region with spatially varying refractive index — e.g. shower glass).
- The phase screen results in a slight corrugation of the wavefront, and consequently the rays will be slightly deflected from their original parallel paths and this will result in spatial variation in the energy flux.
- A generic feature of such light deflection is the developments of caustic surfaces on which the flux is *infinite*.

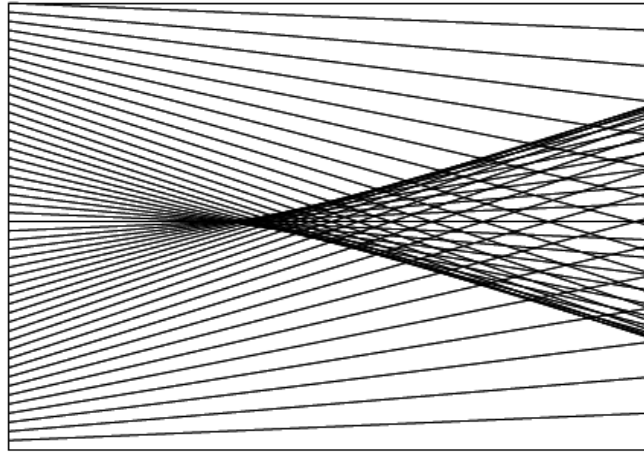
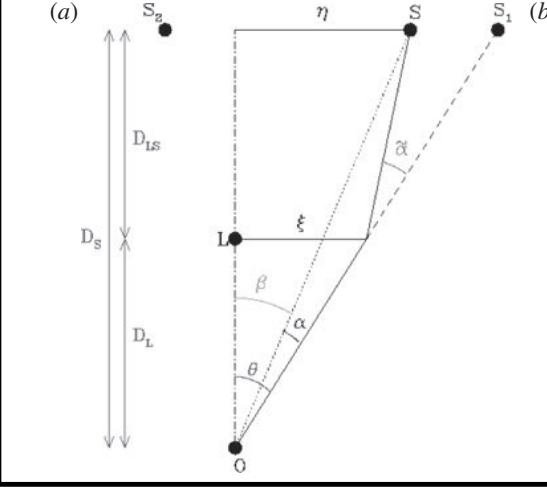


Figure 8.1: Formation of a caustic. The rays illustrated here (propagating left to right) have been subjected to a smoothly varying deflection field. This leads to focusing of rays and formation of a caustic. It is apparent that at each point inside the caustic surface there are three different ray directions, and an observer would see three images of the assumed distant source. The high spatial density of rays just inside the caustic surface correspond to high amplification of the flux.

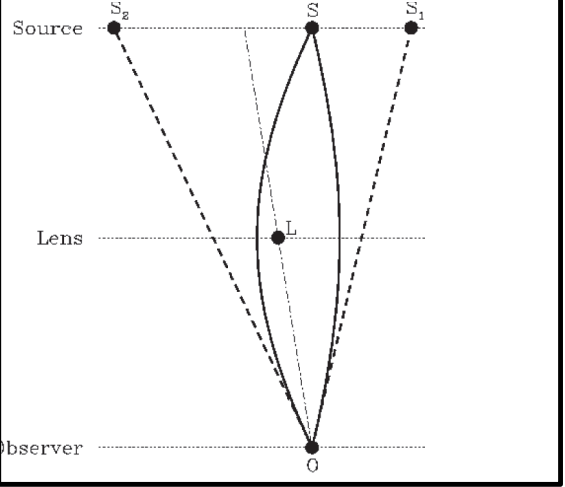
Gravitational lensing has two major advantages that turn it into a versatile cosmological tool :

- its foundation in the theory of gravity is straightforward, and it is sensitive to matter (and energy) inhomogeneities regardless of their internal physical state.
- Under the assumptions that gravitational lenses are weak, move slowly with respect to the cosmological rest frame, and are much smaller than cosmological length scales, the effects of gravitational lensing are entirely captured by a two-dimensional effective lensing potential. (Matthias Bartelmann & Matteo Maturi 1612.06535.pdf)

the deflection of light by a deflector, or lens, of mass M (Wambsgans, 1998).

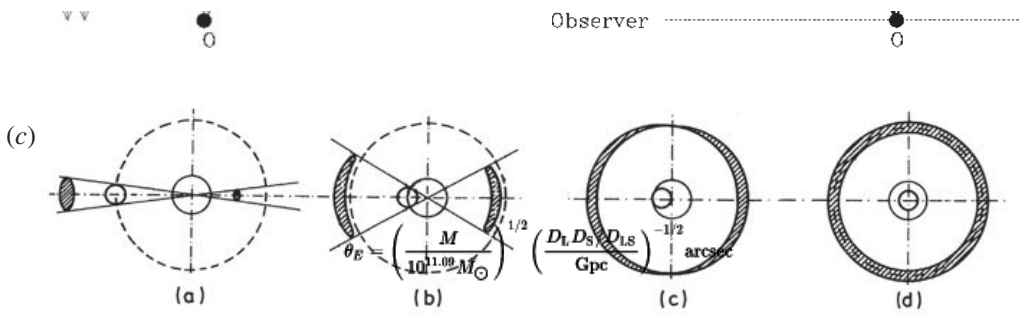


the two light paths from the source to the observer for a point mass



D_s = distance to source
 D_{LS} distance from source to lens
 D_L distance from us to lens

Longair
 Figure
 4.11



- Changes in the appearance of a compact background source as it passes behind a point mass. The dashed circles correspond to the Einstein radius (really an angle). When the lens and the background source are precisely aligned, an Einstein ring is formed with radius equal to the Einstein radius θ_E .

Lensing

- assume -
the overall geometry of the universe is Friedmann--Robertson- Walker metric matter inhomogeneities which cause the lensing are local perturbations.
- Light paths propagating from the source past the lens 3 regimes
- 1) light travels from the source to a point close to the lens through unperturbed spacetime.
- 2) near the lens, light is deflected.
- 3) light again travels through unperturbed spacetime.

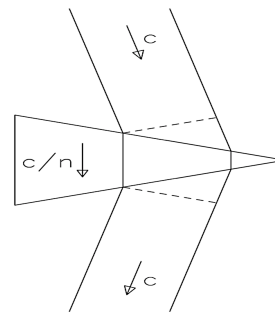
The effect of spacetime curvature on the light paths can be expressed in terms of an effective index of refraction, n , (e.g. Schneider et al. 1992)

$n = 1 - (2/c^2) \phi(r)$; $\phi(r)$ the Newtonian gravitational potential

As in normal optics, for refractive index $n > 1$ light travels slower than in free vacuum.

effective speed of a ray of light in a gravitational field is

$$v = c/n \sim c - (2/c)\phi$$



- The optical properties of a lumpy universe are, are similar to that of a block of glass of inhomogeneous density where the refractive index is $n(r) = (1 - 2\phi(r)/c^2)$ with $\phi(r)$ the *Newtonian gravitational potential*. In an over-dense region, ϕ is negative, so n is slightly greater than unity. In this picture we think of space as being flat, but that the speed of light is slightly retarded in the over-dense region.

Ways of Thinking About Lensing (Kaiser sec 33.5)

- This deflection is just twice what Newtonian theory would give for the deflection of a test particle moving at $v = c$ where we can imagine the radiation to be test particles being pulled by a gravitational acceleration.
- another way to look at this using wave-optics; the inhomogeneity of the mass distribution causes space-time to become curved. The space in an over-dense region is positively curved.

Light rays propagating through the over-density have to go a slightly greater distance than they would in the absence of the density perturbation.

Consequently the wave-fronts get retarded slightly in passing through the over-density and this results in focusing of rays.

- The deflection of light by a **point mass** M due to the bending of space-time amounts to precisely twice that predicted by a Newtonian calculation,
- $\alpha = 4GM / \xi c^2$, (4.28)

ξ is the 'impact parameter' \sim the distance of closest approach of the light ray to the deflector.

As an example, we now evaluate the deflection angle of a point mass M (cf. Fig. 3). The Newtonian potential of the lens is

$$\Phi(b, z) = -\frac{GM}{(b^2 + z^2)^{1/2}}, \quad (5)$$

where b is the impact parameter of the unperturbed light ray, and z indicates distance along the unperturbed light ray from the point of closest approach. We therefore have

$$\vec{\nabla}_{\perp} \Phi(b, z) = \frac{GM \vec{b}}{(b^2 + z^2)^{3/2}}, \quad (6)$$

where \vec{b} is orthogonal to the unperturbed ray and points toward the point mass. Equation (6) then yields the deflection angle

$$\hat{\alpha} = \frac{2}{c^2} \int \vec{\nabla}_{\perp} \Phi dz = \frac{4GM}{c^2 b}. \quad (7)$$

Note that the Schwarzschild radius of a point mass is

$$R_S = \frac{2GM}{c^2}, \quad (8)$$

so that the deflection angle is simply twice the inverse of the impact parameter in units of the Schwarzschild radius. As an example, the Schwarzschild radius of the Sun is 2.95 km, and the solar radius is 6.96×10^5 km. A light ray grazing the limb of the Sun is therefore deflected by an angle $(5.9/7.0) \times 10^{-5}$ radians = $1''.7$.

Narayan and Bartellman 1996

Einstein radius is the scale of lensing (see derivation in Longair pg 118)

- For a point mass it is

$$\theta_E = ((4GM/c^2)(D_{ds}/D_d D_s))^{1/2} \quad (4.29)$$

- or in more useful units

$$\theta_E = (0.9'') M_{11}^{1/2} D_{\text{Gpc}}^{-1/2} \quad (4.32)$$

$$\theta_E = 3 \times 10^{-6} (M/M_{\odot})^{1/2} / D^{-1/2} \text{ Gpc arcsec} .$$

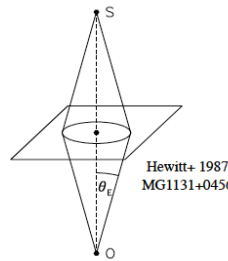
where $D = (D_S D_L / D_{LS})$.

weak lensing preserves surface brightness but changes the apparent solid angle of the source- magnification

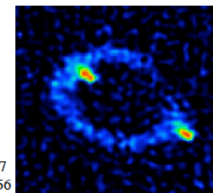
Einstein Ring

When lens, source, and observer lie on the same line get Einstein ring

$$\theta_E = \sqrt{\frac{4GM}{c^2} \frac{D_{LS}}{D_s D_L}}$$



Hewitt+ 1987
MG1131+0456



SDSSJ1430



A. Bolton (JH IFA) for SLACS and NASA/ESA

Condition for formation of lensed image (Σ is surface mass density)

$$\Sigma_{\text{cr}} > [c^2/4\pi G] D_{LS}/D_S D_L \sim 0.35 \text{ g cm}^{-2} / [D]$$

D in Gpc;
see 4.35-4.39

Lensing

- Gravitational deflection of the light ray $\alpha=4\pi v^2/c^2$ (4.43)
- This is exact for a **single isothermal sphere** model of the mass of the lensing object and the Einstein radius is
- $\theta_E=28.8 V_{1000}^2 D_{LS}/D_s$ " (eq 4.44)

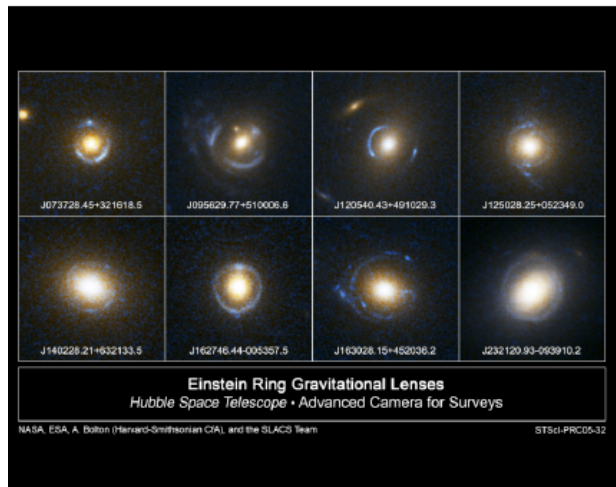
This is a robust expression for estimating the masses of clusters of galaxies (Fort and Mellier, 1994).

So phrased in units of mass

$$M(\theta_E) \approx 4.4 \times 10^{14} M_\odot (r_t/30'')^2 (D_L D_s / D_{LS})$$

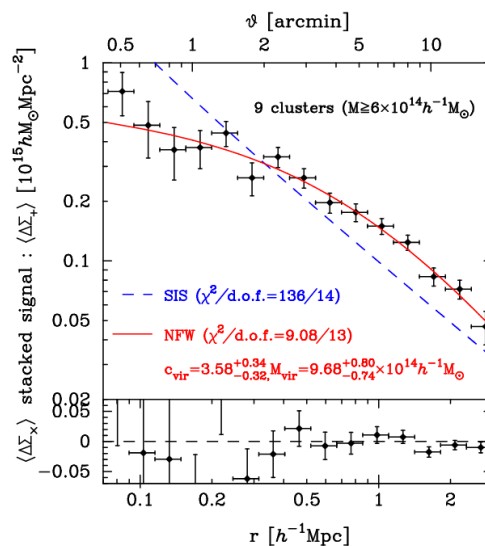
D in units of Gpc

Examples of strong lenses



Weak Lensing (Hoekstra 2013)

- The distortion matrix A can be written in terms of the second derivatives of the deflection potential Ψ
- This transform distorts a circular source into an ellipse with axis ratio $\sim (1 - |g|)/(1 + |g|)$ where $g = \gamma / (1 - \kappa)$ and $2\kappa = \nabla^2 \Psi$
- The observable is thus directly related to g.
- the source is **magnified** by $\mu = 1 / (1 - \kappa)^2 (1 - |g|^2)$,
- $M(\theta_E) = \pi (DL \theta_E)^2 \sum_{cr}$



Okabe et al. (2010).

Weak Lensing (Hoekstra 2013)

- Lensing distorts a circular source into an ellipse with axis ratio

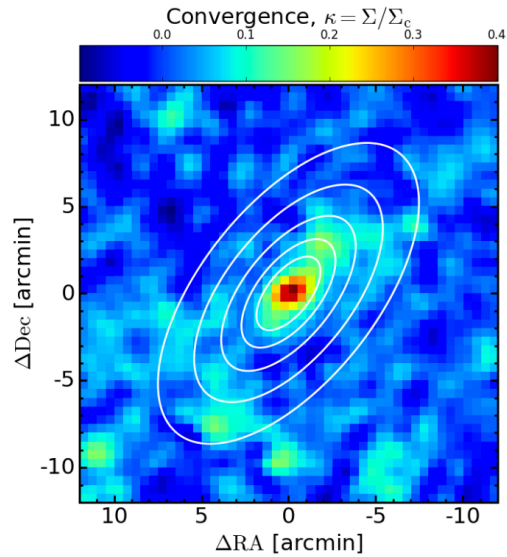
$$\sim (1 - |g|) / (1 + |g|) \text{ where}$$

$$g = \gamma / (1 - \kappa) \text{ and } 2\kappa = \nabla^2 \Psi$$

The gravitational shear γ is directly observable from image ellipticities of background galaxies

- The effect of weak gravitational lensing on background sources is characterized by the convergence, κ , and the shear γ
- The convergence causes an isotropic magnification due to lensing and is defined as the surface mass density Σ in units of the critical surface density for lensing, $\kappa = \Sigma / \Sigma_c$
- the magnification is

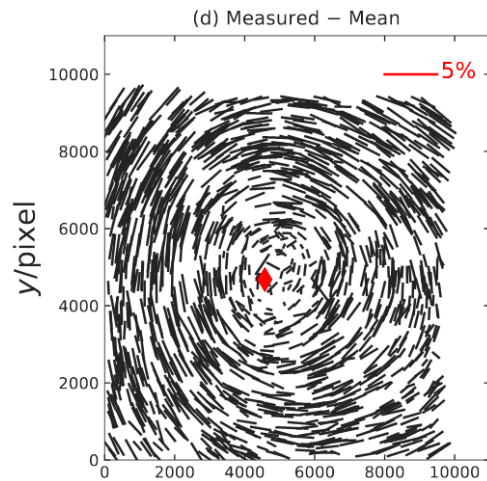
$$\mu = 1 / (1 - \kappa)^2 (1 - |g|^2) \text{ (Kaiser \& Squires 1993)}$$



Umetsu et al. (2018).

Large Scale Mass Distribution

- Cluster shear measurements
Dietrich et al 2019



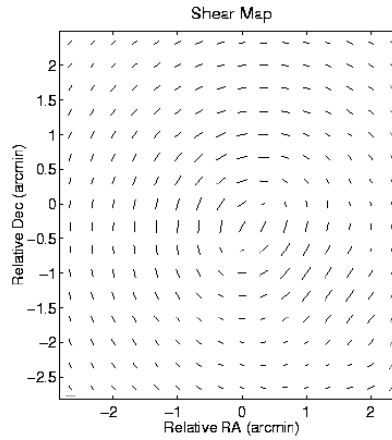
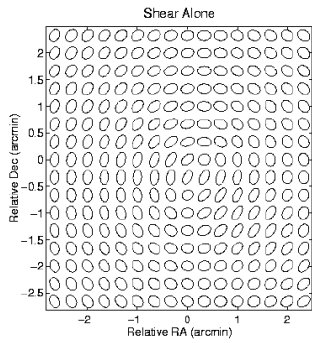
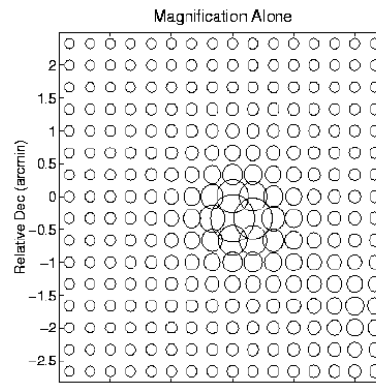
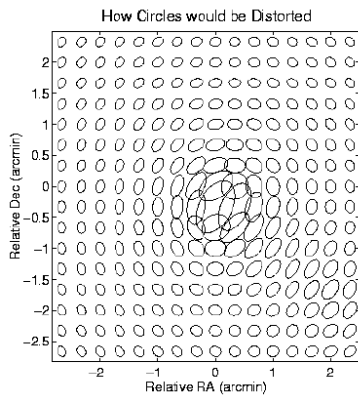
Hoekstra 2008 Texas Conference Gravitational lensing



Inhomogeneities in the mass distribution distort the paths of light rays, resulting in a remapping of the sky. This can lead to spectacular lensing examples...

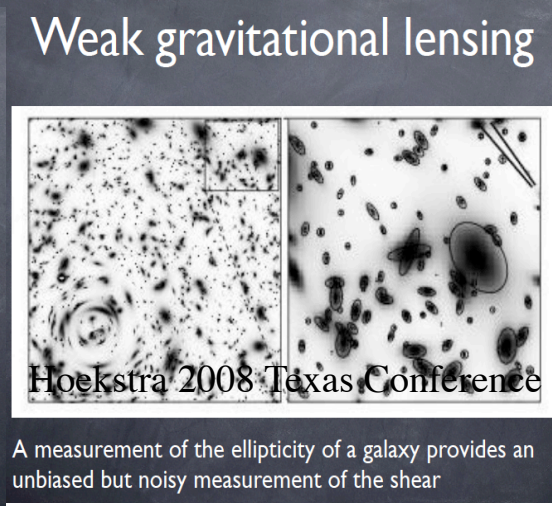
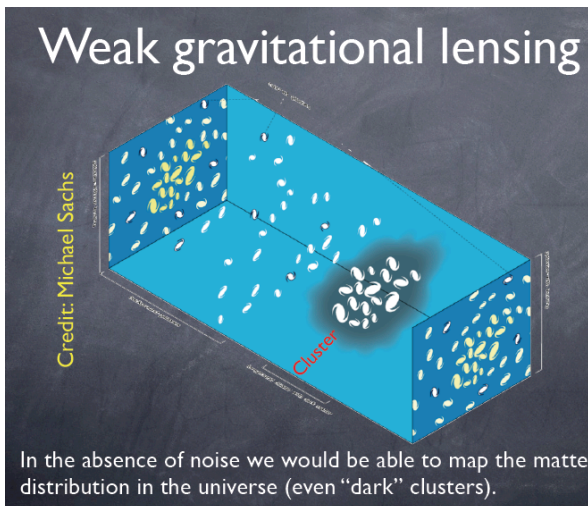
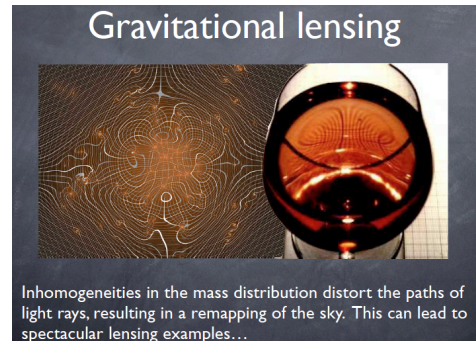


From George F. Smoot



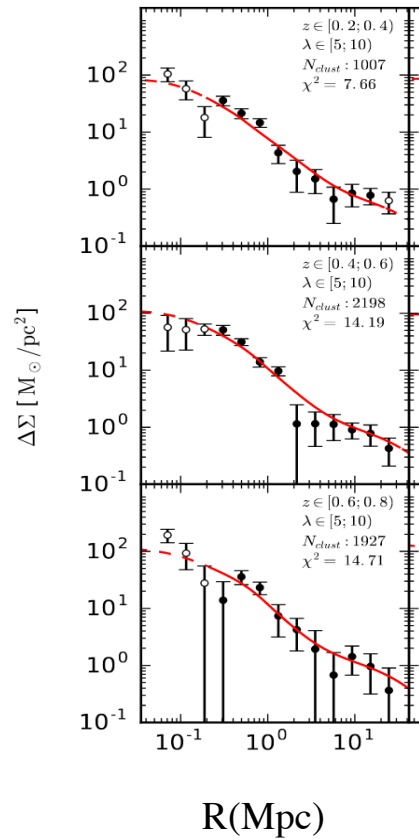
Weak Lensing

- Look for the distortion of the shape of the background objects



Recent Results

- The DES has produced a very large number of cluster weak lensing signals.(8,000 clusters) to $z \sim 0.8$
- While each one is very noisy they can be stacked in mass, redshift to derive statistical results (Melchior et al 1610.06890.pdf) on cluster surface mass profiles.

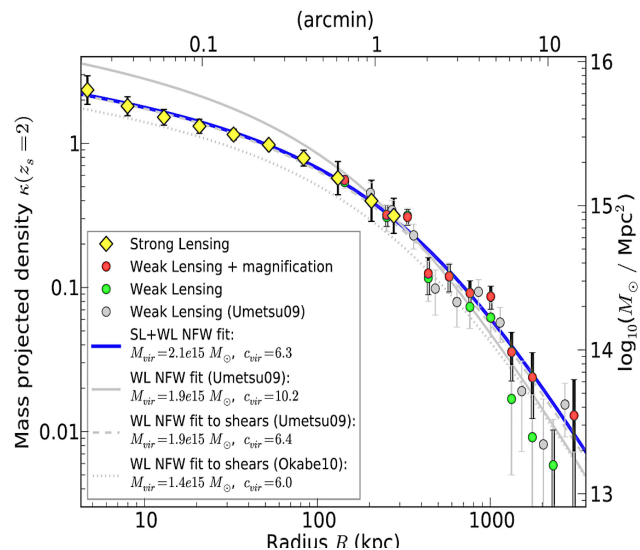


Recent Results

- Detailed lensing studies of >70 clusters have now been done (e.g. CLASH project [2018ApJ...860..104U](#) Umetsu, K et al Canadian Cluster Comparison Project Hoekstra et al 2015MNRAS.449..685, Subaru data Niikura et al 1504.01413.pdf)
- Can combine strong and weak lensing

Results, in general, are consistent with NFW density profile

$$\rho_{\text{NFW}}(r) = \rho_c / (r/r_s)(1+r/r_s)^2$$



NFW Profile

- Stacked mass profile of 50 clusters compared to a NFW profile (Niikura et al 2016)

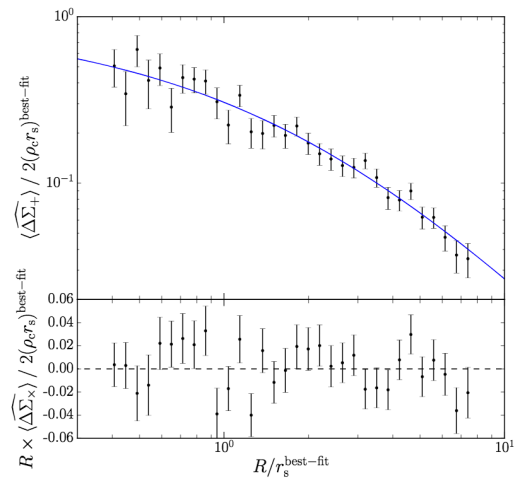
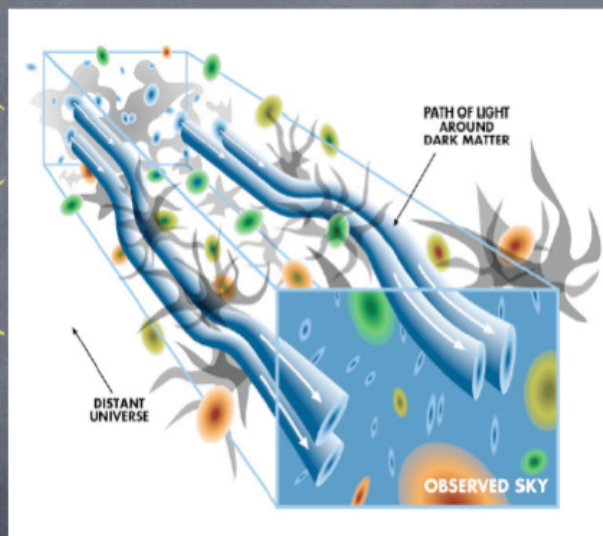


Figure 6. *Upper panel:* The stacked detection profile measured from 50

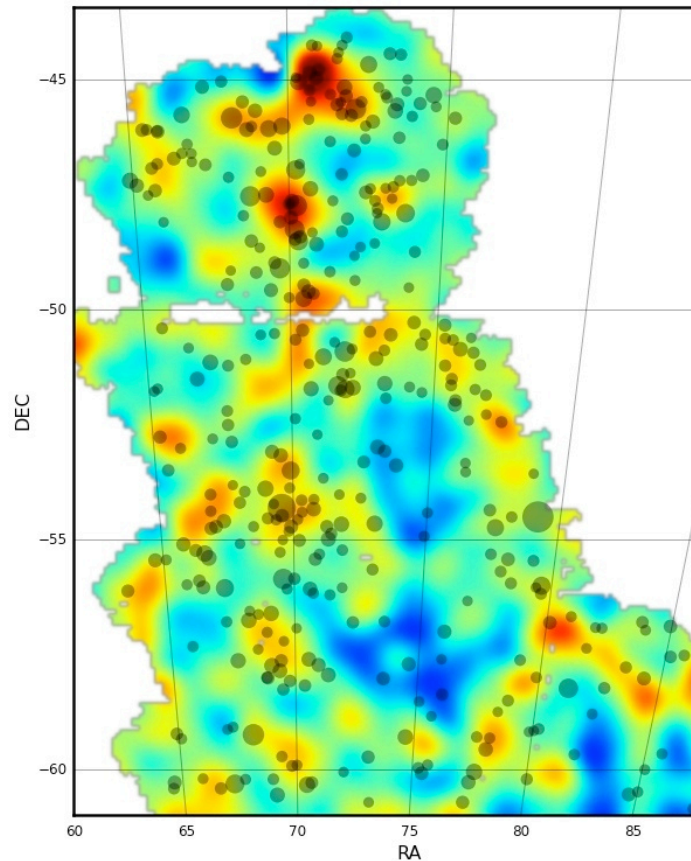
Cosmic shear

Credit: Tyson et al. (2000)

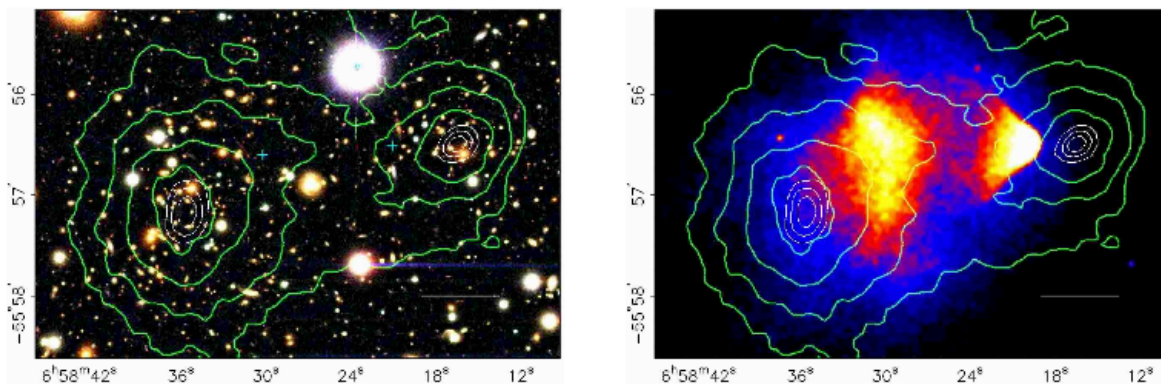


Cosmic shear is the lensing of distant galaxies by the overall distribution of matter in the universe: it is the most “common” lensing phenomenon.

- The detailed distribution of dark matter traced across a large area of sky: yellow and red represent relatively dense regions of dark matter and the black circles represent galaxy clusters (Chang et al 2015)



Lensing and Dark Matter



- Left panel (Clowe et al 2003) optical imaging and mass contours from lensing
- Right panel is the x-ray image with the lensing contours

X-rays from Clusters of Galaxies

- The baryons *thermalize* to $> 10^6$ K making clusters strong X-ray sources- the potential energy of infall is converted into kinetic energy of the gas.
- Most of the baryons in a cluster are in the X-ray emitting plasma - only 10-20% are in the galaxies.
- Clusters of galaxies are self-gravitating accumulations of dark matter which have trapped hot plasma (intracluster medium - ICM) and galaxies: (the galaxies are the least massive constituent)

What we try to measure with X-ray Spectra

- From the x-ray spectrum of the gas we can measure a mean temperature, a redshift, and abundances of the most common elements (heavier than He).
- With good S/N we can determine whether the spectrum is consistent with a single temperature or is a sum of emission from plasma at different temperatures.
- Using symmetry assumptions the X-ray surface brightness can be converted to a measure of the ICM density.

What we try to measure II

If we can measure the temperature and density at different positions in the cluster then assuming the plasma is in hydrostatic equilibrium we can derive the gravitational potential and hence the amount and distribution of the dark matter.

There are two other ways to get the gravitational potential :

- The galaxies act as test particles moving in the potential so their velocities and positional distribution provides a measure of total mass (Viral theorem)
- The gravitational potential acts as a lens on light from background galaxies (previous slides).

Why do we care ?

Cosmological simulations predict distributions of masses.

If we want to use X-ray selected samples of clusters of galaxies to measure cosmological parameters then we must be able to relate the observables (X-ray luminosity and temperature) to the theoretical masses.

Theoretical Tools

- Physics of hot plasmas
 - Bremsstrahlung
 - Collisional equilibrium
 - Atomic physics

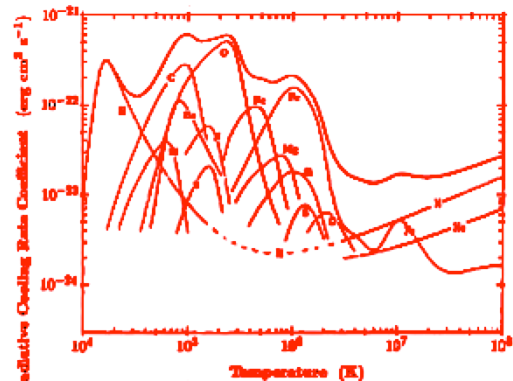
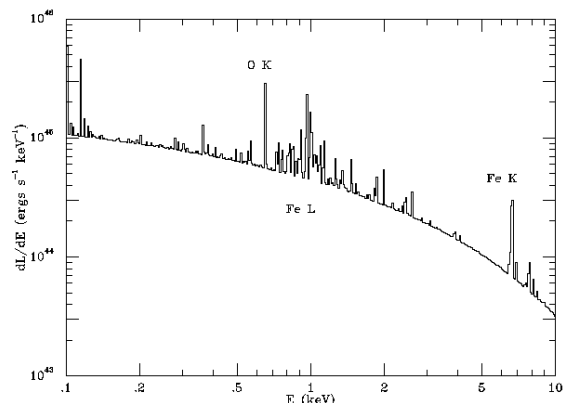
Physical Processes

- Continuum emission
 - Thermal bremsstrahlung, $\sim \exp(-h\nu/kT)$
 - Bound-free (recombination)

- Line Emission
(line emission)
 $L_\nu \sim \epsilon_\nu(T, \text{abund}) (n_e^2 V)$

Line emission dominates cooling at $T < 10^7$ K

Bremsstrahlung at higher temperatures

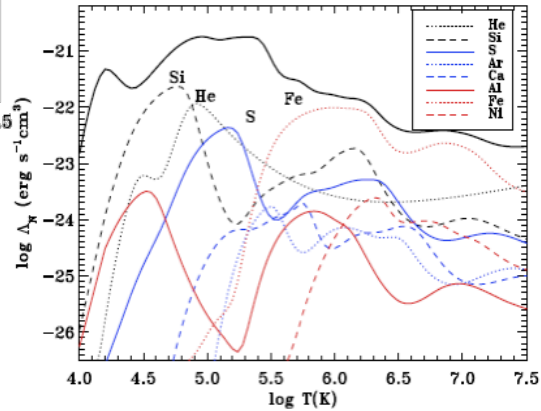
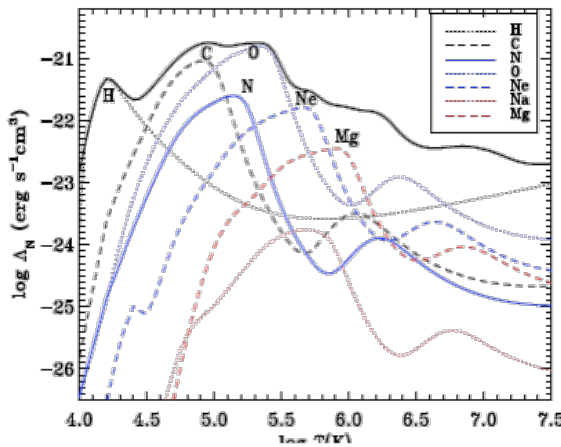


$$\epsilon(\nu) = \frac{16 e^6}{3 m_e c^2} \left(\frac{2\pi}{3 m_e k_B T_X} \right)^{1/2} n_e n_i Z^2 g_{ff}(Z, T_X, \nu) \exp\left(\frac{-h\nu}{k_B T_X}\right)$$

Cooling rate of hot plasma as a function of the plasma temperature. The contribution to the cooling of different important abundant elements is indicated (Böhringer and Henke 1989). Most of

Cooling Function Λ

Notice the 5 order of magnitude range in the various components of Λ in as a function of kT

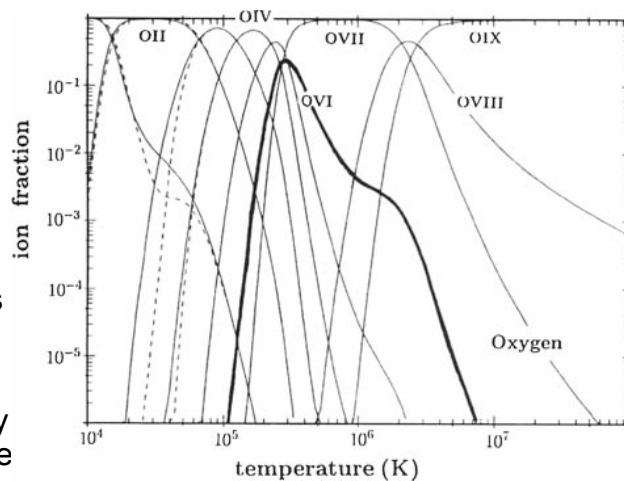


- Cooling function is the emissivity per unit volume at a fixed density as a function of temperature
- The two panels show a different set of elements
- The black curve is the sum of line and continuum cooling

Fig. 2. Contributions of different elements to the cooling curve are given. Each of the plots shows a different set of elements. Important peaks are labelled with the name of the element. The total cooling curve (black solid line) is an addition of the individual elemental contributions.

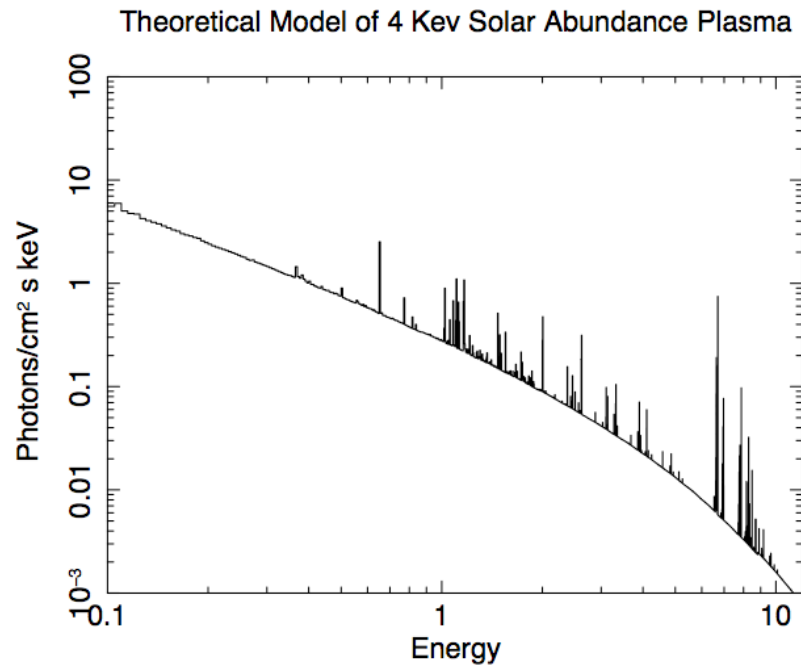
Cluster Plasma Parameters

- Electron number density $n_e \sim 10^{-3} \text{ cm}^{-3}$ in the center with density decreasing as $n_e \sim r^{-2}$
- $10^6 < T < 10^8 \text{ k}$
- Mainly H, He, but with heavy elements (O, Fe, ..)
- Mainly emits X-rays
- $10^{42} < L_x < 10^{45.3} \text{ erg/s}$, most luminous extended X-ray sources in Universe
- 'Age' $\sim 2\text{-}10 \text{ Gyr}$
- Mainly ionized, but not completely
e.g. He and H-like ions of the abundant elements (O...Fe) exist in thermal equilibrium



Ion fraction for oxygen vs electron temperature

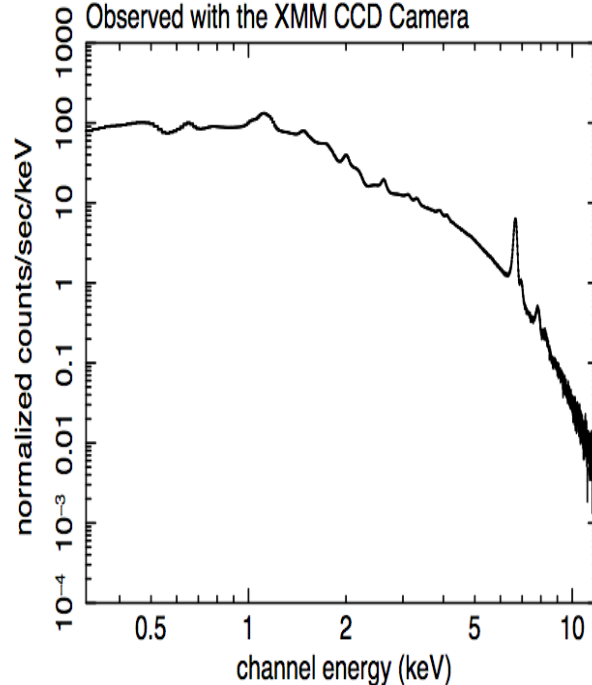
- Theoretical model of a collisionally ionized plasma $kT=4$ keV with solar abundances
- The lines are 'narrow'
- Notice dynamic range of 10^4



X-ray Spectra Data

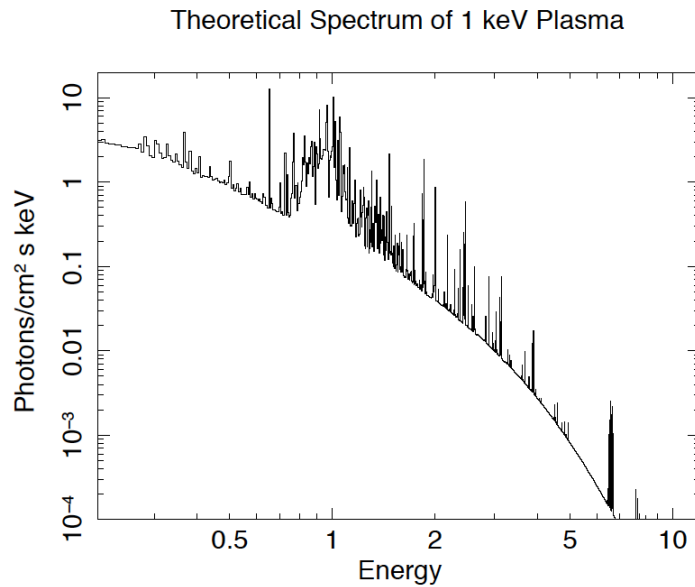
- For hot ($kT > 3 \times 10^7$ k) plasmas the spectra are continuum dominated- most of the energy is radiated in the continuum
- (lines broadened by the detector resolution)

Simulated X-ray Spectrum of a $kT=4$ keV Plasma with Solar Abundance Observed with the XMM CCD Camera

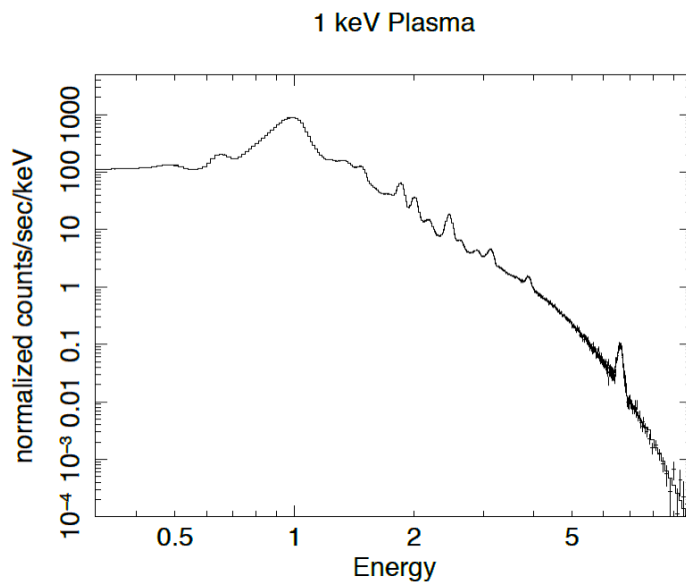


1 keV Plasma

- **Theoretical model** of a collisionally ionized plasma $kT=1$ keV with solar abundances
- The lines are 'narrow'
- Notice dynamic range of 10^5

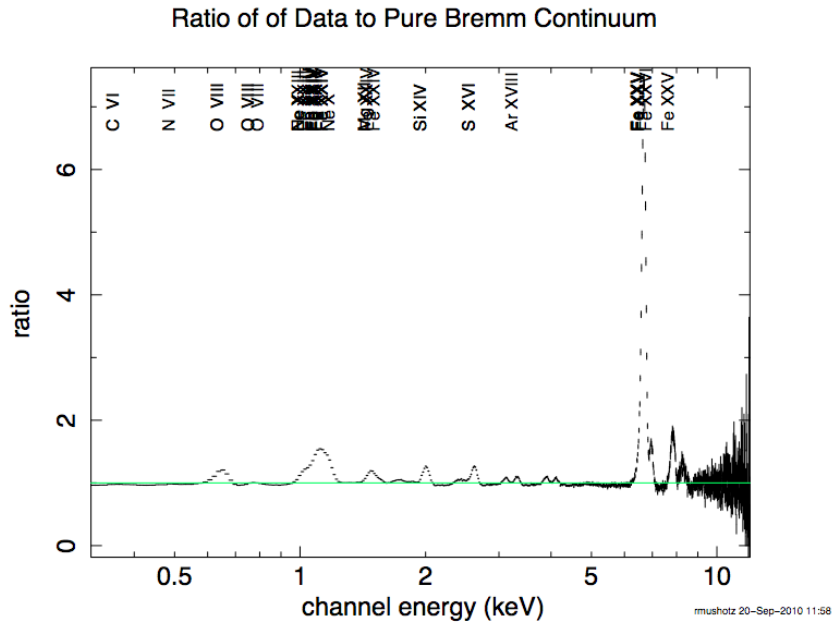


- **Observational (CCD) data** for a collisionally ionized plasma $kT=1$ keV with solar abundances
- Notice the very large blend of lines near 1 keV- L shell lines of Fe
- **Notice dynamic range of 10^7**
- Will have more on this subject when we discuss chemical abundances



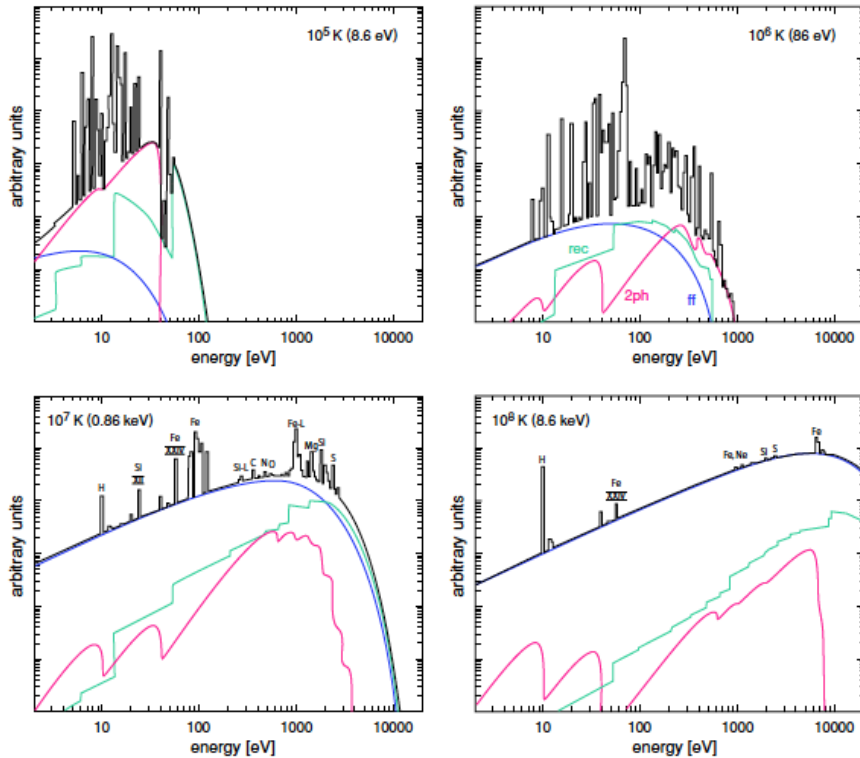
Collisionally Ionized Equilibrium Plasma

- Ratio of model to a 'pure' H/He plasma $kT=4$ keV
- This plot is designed to show the lines
- Notice the very large EW of the He/H-like Fe complex



Strong Temperature Dependence of Spectra

- Line emission
- Brems (black)
- Recombination (green)
- 2 photon red



How to measure the mass of clusters? Longair sec 4.4

ICM in (most) clusters close to gravitational equilibrium: outward gas pressure \approx inward gravitational pull

Hydrostatic Equilibrium

$$\frac{1}{\rho_{gas}} \nabla P_{gas} = -\nabla \Phi$$

Poisson's Equation

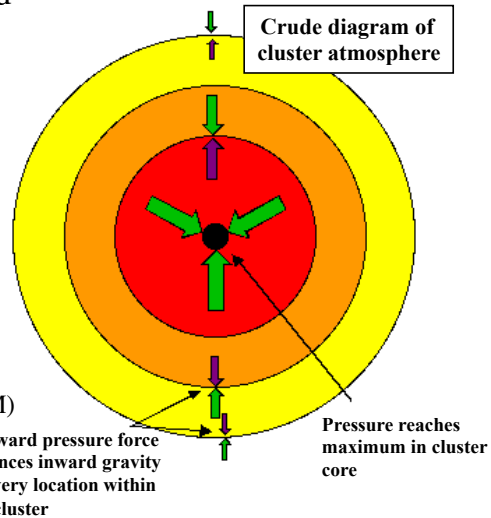
$$\nabla^2 \Phi = 4\pi G \rho_{grav}$$

Spherical Symmetry

$$\frac{1}{\rho_{gas}} \frac{dP}{dr} = -\frac{d\Phi}{dr} = -\frac{GM(r)}{r^2}$$

luminous matter:
temp., density

total mass
(including DM)



X-ray obs.

Cluster gas pressure profile:

- Separable problem
 - measure gas density profile
 - measure gas temperature profile
- Need X-ray observations

Patrick Koch

- Next paper- How clusters can constrain the nature of dark matter

Constraints on the Self-Interaction Cross Section of Dark Matter from Numerical Simulations of the Merging Galaxy Cluster 1E 0657-56 **Authors:**

[Randall, Scott W.](#); [Markevitch, Maxim](#); [Clowe, Douglas](#);

[Gonzalez, Anthony H.](#); [Bradač, Maru](#)

[2008ApJ...679.1173R](#)

Assumptions

- Gas is in equilibrium- what are the relevant time scales

Another good review article is Astron Astrophys Rev (2010) 18:127–196 X-ray spectroscopy of galaxy clusters: studying astrophysical processes in the largest celestial laboratories Hans Böhringer and Norbert Werner

Relevant Time Scales- see Longair pg 301

- The **equilibration timescales between protons and electrons** is $t(p,e) \sim 2 \times 10^8$ yr at an 'average' location
- In collisional ionization equilibrium population of ions is directly related to temperature**

$$\tau(1,2) = \frac{3m_1\sqrt{2\pi}(kT)^{3/2}}{8\pi\sqrt{m_2}n_2Z_1^2Z_2^2e^4\ln\Lambda}$$

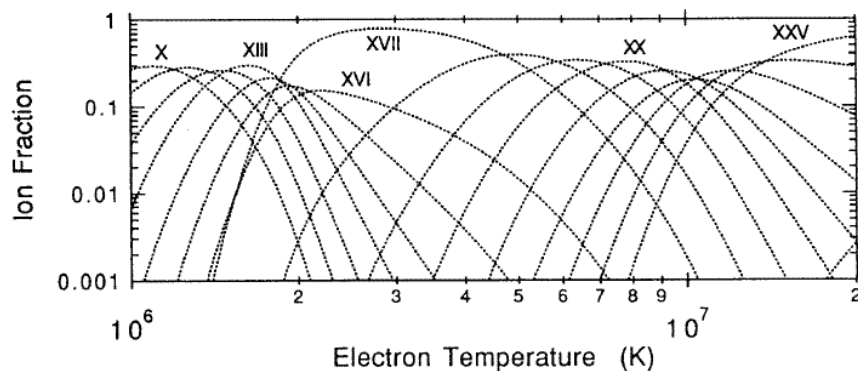
$$\ln\Lambda \equiv \ln(b_{\max}/b_{\min}) \approx 40$$

$$\tau(e,e) \approx 3 \times 10^5 \left(\frac{T}{10^8 \text{ K}} \right)^{3/2} \left(\frac{n_e}{10^{-3} \text{ cm}^{-3}} \right)^{-1} \text{ yr}$$

$$\tau(p,p) = \sqrt{m_p/m_e} \tau(e,e) \approx 43\tau(e,e)$$

$$\tau(p,e) = (m_p/m_e)\tau(e,e) \approx 1800\tau(e,e)$$

Ion fraction for Fe vs electron temperature



Mean Free Path for Collisions/ Energy

- Mean-free-path $\lambda_e \sim 20$ kpc
< 1% of cluster size

$$\lambda_p \approx \lambda_e = \frac{3^{3/2} (kT)^2}{8\sqrt{\pi} n_e e^4 \ln \Lambda}$$

$$\approx 23 \left(\frac{T}{10^8 \text{ K}} \right)^2 \left(\frac{n_e}{10^{-3} \text{ cm}^{-3}} \right)^{-1} \text{ kpc}$$

Assumptions

- At $T > 3 \times 10^7$ K the major form of energy emission is thermal bremsstrahlung continuum
- $\epsilon \sim 3 \times 10^{-27} T^{1/2} n^2$ ergs/cm³/sec; emissivity of gas
- - how long does it take a parcel of gas to lose its energy?
- $\tau \sim nkT/\epsilon \sim 8.5 \times 10^{10} \text{ yrs} (n/10^{-3})^{-1} T_8^{1/2}$
- At lower temperatures line emission is important

How Did I Know This??

- Why do we think that the emission is thermal bremsstrahlung?
 - X-ray spectra are consistent with model
 - continuum and line ratios
 - X-ray 'image' is also consistent
 - Derived physical parameters 'make sense'
 - Other mechanisms 'do not work' (e.g. spectral form not consistent with black body, synchrotron from a power law: presence of x-ray spectral lines of identifiable energy argues for collisional process; ratio of line strengths (e.g. He to H-like) is a measure of temperature which agrees with the fit to the continuum)

Assumptions

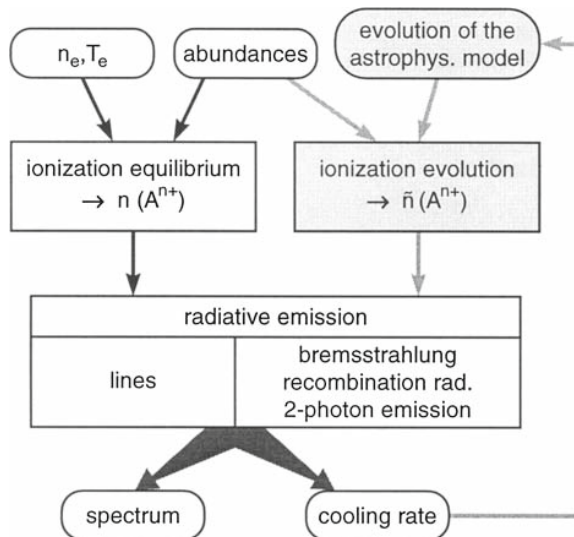
- The physical conditions are consistent with the assumptions

Physical Conditions in the Gas

- the elastic collision times for (ions and electrons) in the intracluster gas are much shorter than the time scales for heating or cooling , and the gas can be treated as a fluid. The time required for a sound wave in the intracluster gas to cross a cluster is given by
- $T_s \sim 6.6 \times 10^8 \text{ yr } (T_{\text{gas}}/10^8)^{1/2} (D/\text{Mpc})$
 - thus on timescale of Gyr system should be in pressure equilibrium "if nothing happens"
- (remember that for an ideal gas $v_{\text{sound}} = \sqrt{(\gamma P/\rho_g)}$ (P is the pressure, ρ_g is the gas density, $\gamma=5/3$ is the adiabatic index for a monoatomic ideal gas)

Why is Gas Hot

- To first order if the gas were cooler it would fall to the center of the potential well and heat up
 - If it were hotter it would be a wind and gas would leave cluster
 - Idea is that gas shocks as it 'falls into' the cluster potential well from the IGM
 - Is it 'merger' shocks (e.g. collapsed objects merging)
 - Or in fall (e.g. rain)
- BOTH**



How do Clusters Form- Mergers

- As time progresses more and more objects come together- merge

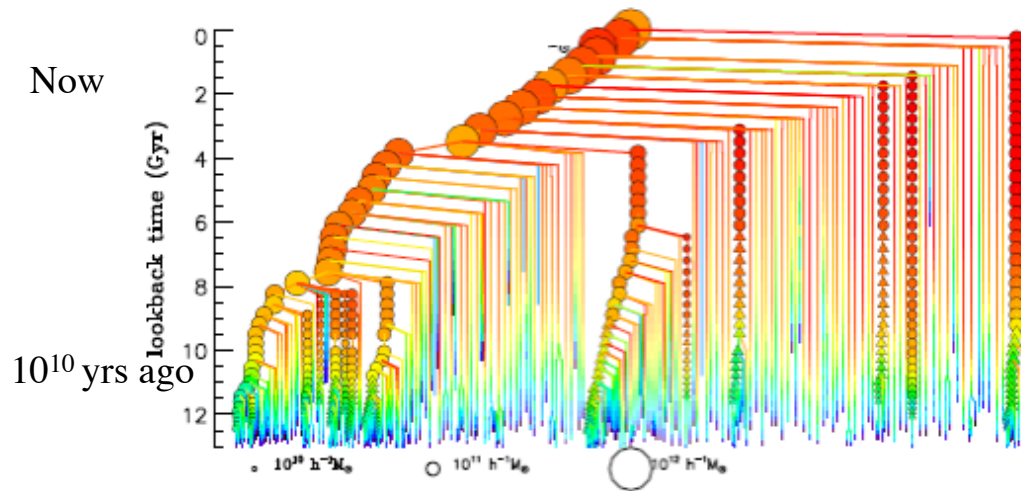
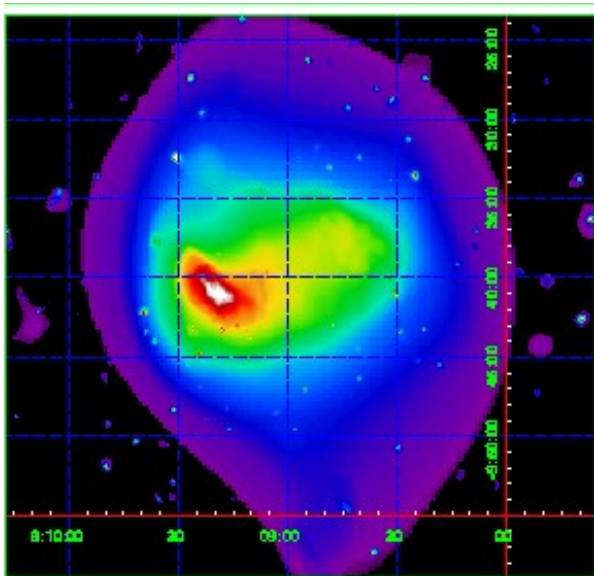
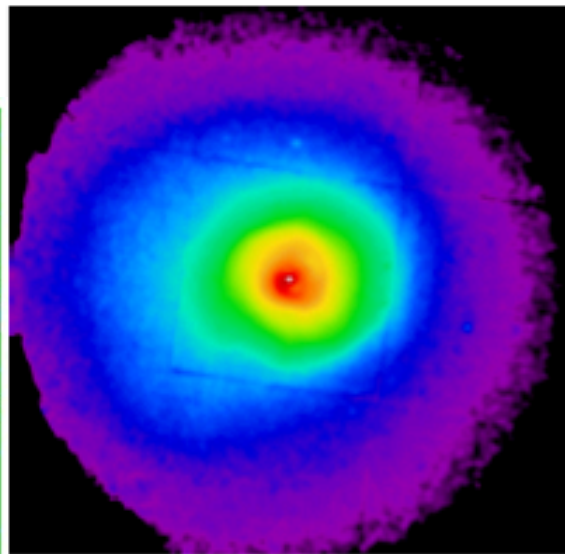


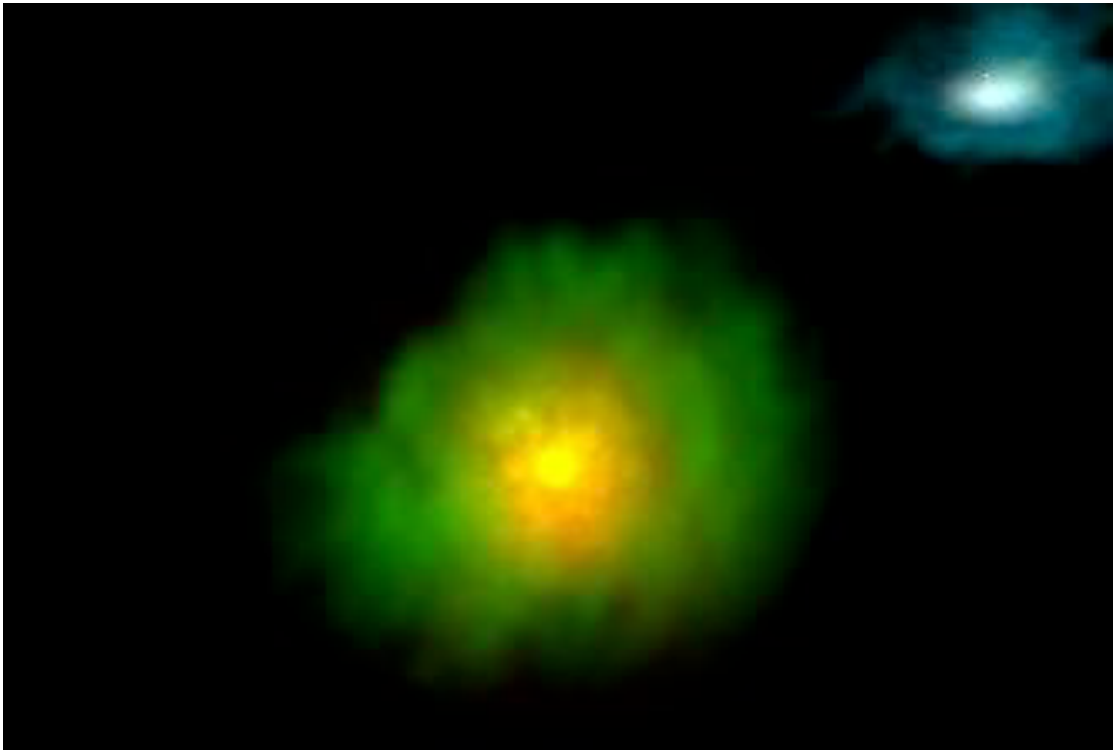
Figure 1. BOG merger tree. Symbols are colour-coded as a function of B - V colour and their area scales with the stellar mass. Only progenitors more massive than $10^{10} M_{\odot} h^{-1}$ are shown with symbols. Circles are used for galaxies that reside in the FOF group inhabited by the main branch. Triangles show galaxies that have not yet joined this FOF group.



Merger



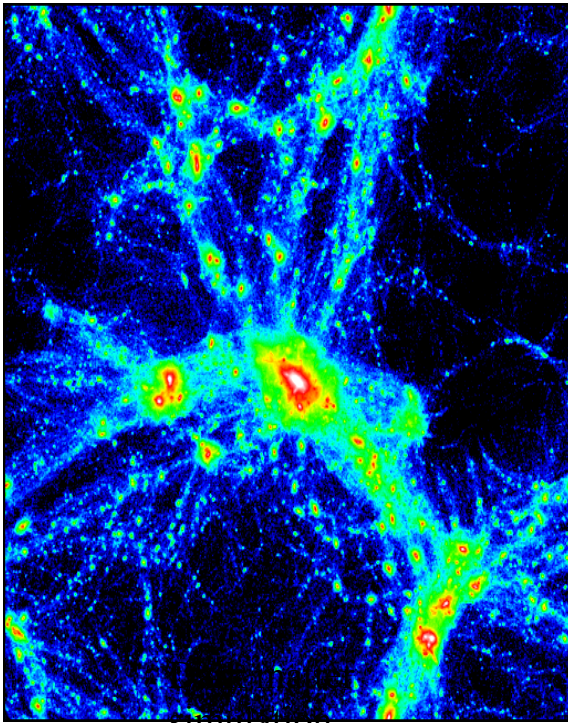
NOT A
MERGER



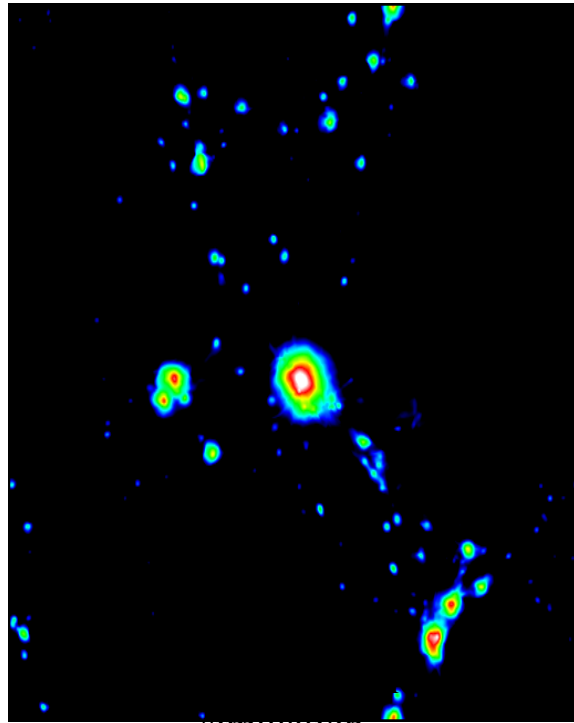
Galaxy Cluster Merger

Rubens Machado, Gastão Lima Neto
IAG-USP
2012

Comparison of dark matter and x-ray cluster and group distribution
 every bound system visible in the numerical simulation is detected in the x-ray band - bright regions are massive clusters, dimmer regions groups,



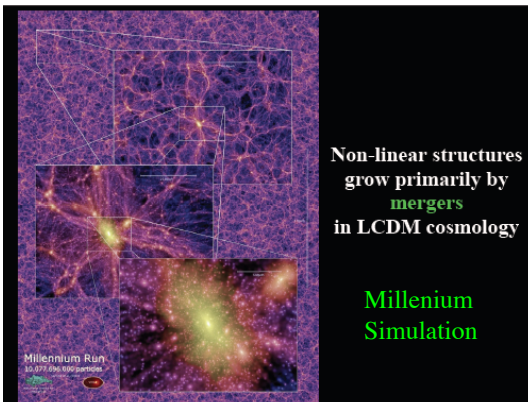
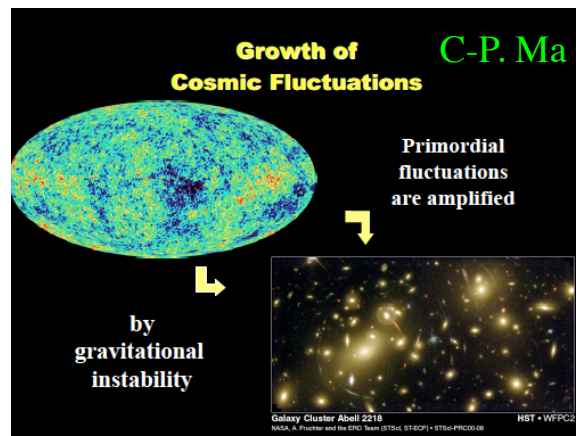
Simulation



Simulation

Formation

- Galaxy clusters form through gravitational collapse, driven by dark matter (~80% of their total mass)
- In the hierarchical scenario more massive objects form at later times: clusters of galaxies are produced by the gravitational merger of smaller systems, such as groups and sub-clusters



Extreme Merger

- Bullet cluster (1E0657)
- Allen and Million
- The assumptions we have given are NOT satisfied

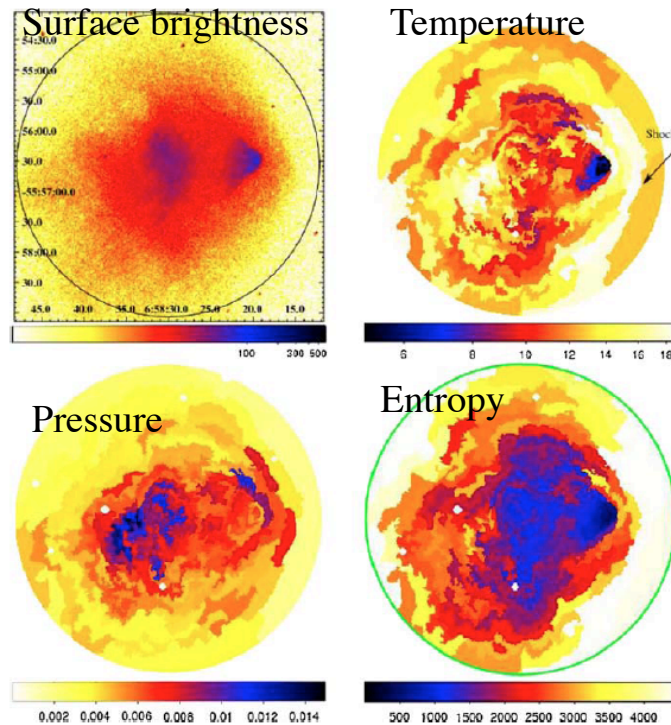


Fig. 16 Thermodynamic maps for the ICM of the "bullet cluster", 1E0657-56 (Million and Allen 2008)

Hydrostatic Equilibrium Kaiser 19.2

- Equation of hydrostatic equil

$$\nabla P = -\rho_g \nabla \phi(\mathbf{r})$$

where $\phi(\mathbf{r})$ is the gravitational potential of the cluster (which is set by the distribution of matter)

P is the gas pressure

ρ_g is the gas density

However the fundamental assumption is that the total pressure IS gas pressure and that the contribution of turbulence, magnetic fields, cosmic rays etc is negligible

Use of X-rays to Determine Mass

- X-ray emission is due to the combination of thermal bremsstrahlung and line emission from hot gas
- The gas "should be" in equilibrium with the gravitational potential (otherwise flow out or in)
- density and potential are related by Poisson's equation

$$\nabla^2 \phi = 4\pi\rho G$$

- and combining this with the equation of hydrostatic equilibrium

$$\nabla \cdot \left(\frac{1}{\rho} \nabla P \right) = -\nabla^2 \phi = -4\pi G \rho$$

gives for a spherically symmetric system

$$\left(\frac{1}{\rho_g} \right) \frac{dP}{dr} = -\frac{d\phi(r)}{dr} = \frac{GM(r)}{r^2}$$

With a little algebra and the definition of pressure - the **total cluster mass** (dark and baryonic) can be expressed as

$$M(r) = -\left(\frac{kT_g(r)}{\mu G m_p} \right) r \left(\frac{d \ln T}{dr} + \frac{d \ln \rho_g}{dr} \right)$$

k is Boltzmann's constant, μ is the mean mass of a particle and m_H is the mass of a hydrogen atom. Every thing is observable

The temperature T_g from the spatially resolved spectrum

The density ρ_g from the knowledge that the emission is due to bremsstrahlung

And the scale size, r , from the conversion of angles to distance

see Longair eq 4.2-4.6

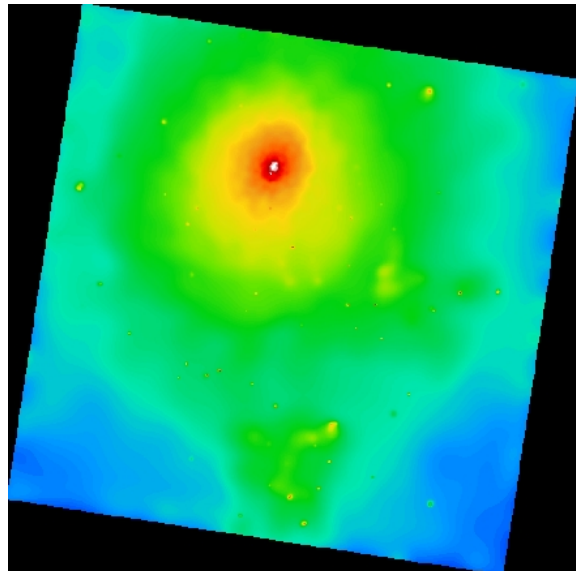
73

- density and potential are related by Poisson's equation

$$\nabla^2 \phi = 4\pi\rho G$$

- and combining this with the equation of hydrostatic equilibrium

$$\nabla \cdot \left(\frac{1}{\rho} \nabla P \right) = -\nabla^2 \phi = -4\pi G \rho \quad (\text{eq 4.3 in Longair})$$



Hydrodynamics--see Longair ch 4.2

$$\frac{\partial \rho}{\partial t} + \nabla \cdot (\rho \mathbf{v}) = 0 \quad \text{mass conservation (continuity)}$$

$$\rho \frac{D\mathbf{v}}{Dt} + \nabla P + \rho \nabla \phi = 0 \quad \text{momentum conservation (Euler)}$$

$$\rho T \frac{Ds}{Dt} = H - L \quad \text{entropy (heating \& cooling)}$$

$$P = \frac{\rho k T}{\mu m_p} \quad \text{equation of state}$$

Add viscosity, thermal conduction, ...

Add magnetic fields (MHD) and cosmic rays

Gravitational potential ϕ from DM, gas, galaxies

Deriving the Mass from X-ray Spectra

Ch 4.4 Longair

For spherical symmetry this reduces to

$$(1/\rho_g) dP/dr = -d\phi(r)/dr = GM(r)/r^2$$

With a little algebra and the definition of pressure - the total cluster mass can be expressed as (eqs 4.17-4.19 in Longair)

$$GM(r) = k T_g(r) / (\mu G m_p) r (d \ln T / dr + d \ln \rho_g / dr)$$

k is Boltzmann's constant, μ is the mean mass of a particle and m_H is the mass of a hydrogen atom

Every thing is observable

The temperature T_g from the spatially resolved spectrum

The density ρ_g from the knowledge that the emission is due to bremsstrahlung and the x-ray image

And the scale size, r , from the conversion of angles to distance

How to Obtain Gas Density

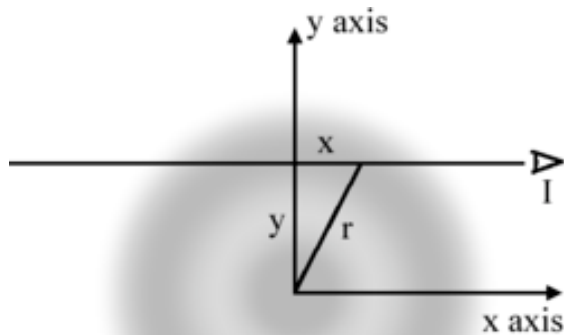
- De-project X-ray surface brightness profile $I(R)$ to obtain gas density vs. radius, $\rho(r)$

$$I_v(b) = \int_{b^2}^{\infty} \frac{\epsilon_v(r) dr^2}{\sqrt{r^2 - b^2}}$$

$$\epsilon_v(r) = -\frac{1}{\pi} \frac{d}{dr^2} \int_{r^2}^{\infty} \frac{I_v(b) db^2}{\sqrt{b^2 - r^2}} = \Lambda_v[T(r)] n_e^2(r)$$

- Where Λ is the cooling function and n_e is the gas density (subtle difference between gas density and electron density because the gas is not pure hydrogen)
- De-project X-ray spectra in annuli $T(r)$
- Pressure $P = \rho kT / (\mu m_p)$
- The mass in gas is $M_{\text{gas}}(< r) = 4\pi \int_0^r r'^2 dr' \rho_{\text{gas}}(r')$

A geometrical interpretation of the Abel transform in two dimensions. An observer (I) looks along a line parallel to the x-axis a distance y above the origin. What the observer sees is the projection (i.e. the integral) of the circularly symmetric function $f(r)$ along the line of sight. The function $f(r)$ is represented in gray in this figure. The observer is assumed to be located infinitely far from the origin so that the limits of integration are $\pm\infty$



- $I(R)$ is the **projected** luminosity surface brightness, **$j(r)$ is the 3-D** luminosity density (circular images- if image is elliptical no general solution)

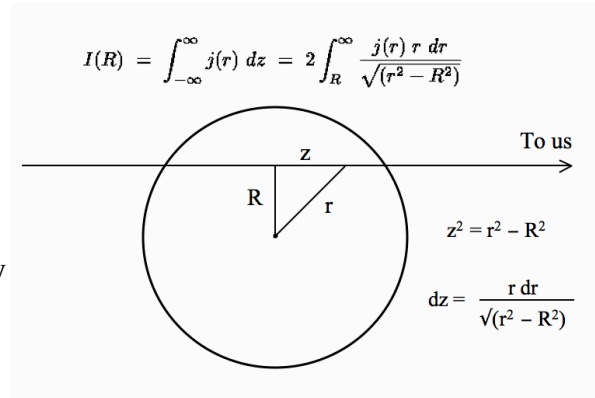
Density Profile- Longair 4.22

$$j(r) = -1/\pi \int_R^\infty dI/dR / \sqrt{R^2 - r^2}$$

this is an Abel integral which has only a few analytic solutions

Simple power law models $I(R) = r^{-\alpha}$

$$\text{then } j(r) = r^{-\alpha-1}$$



generalized King profile with surface brightness

$$I(r) = I(0)(1 + (r/r_c)^2)^{-5/2}$$

gives a density law $\rho(r) = \rho(0)(1 + (r/r_c)^2)^{-3/2}$ where $r_c = 3\sigma / \sqrt{4\pi G \rho_c}$

79

Sarazin sec 5

The gas distributions in clusters can be derived directly from observations of the X-ray surface brightness of the cluster, if the shape of the cluster is known and if the X-ray observations are sufficiently detailed and accurate. This method of analysis also leads to a method for determining cluster masses (Section 5.5.5). The X-ray surface brightness at a photon frequency ν and at a projected distance b from the center of a spherical cluster is

$$I_\nu(b) = \int_{b^2}^{\infty} \frac{\epsilon_\nu(r) dr^2}{\sqrt{r^2 - b^2}}, \quad (5.80)$$

where ϵ_ν is the X-ray emissivity. This Abel integral can be inverted to give the emissivity as a function of radius,

$$\epsilon_\nu = -\frac{1}{2\pi r} \frac{d}{dr} \int_{r^2}^{\infty} \frac{I_\nu(b) db^2}{\sqrt{b^2 - r^2}}. \quad (5.81)$$

Density Profile

- a simple model (the β model) fits the *surface brightness* well outside the core

$$- S(r) = S(0)(1+r/a)^2)^{-3\beta+1/2} \text{ ph/cm}^2/\text{sec/solid angle}$$

- Is analytically invertible (inverse Abel transform) to the *density profile*
 $\rho(r) = \rho(0)(1+(r/a)^2)^{-3\beta/2}$

The conversion function from $S(0)$ to $\rho(0)$ depends on the detector

The quantity 'a' is a scale factor- sometimes called the core radius

β is a free parameter

- The Abel transform, \mathcal{A} , is an integral transform used in the analysis of spherically symmetric or axially symmetric functions. The Abel transform of a function $f(r)$ is given by:

$$f(r) = 1/p \int_r^\infty dF/dy \, dy / \sqrt{(y^2 - r^2)}$$

- In image analysis the reverse Abel transform is used to calculate the emission function given a projection (i.e. a scan or a photograph) of that emission function.
- In general the integral is not analytic

Surface Brightness Profiles

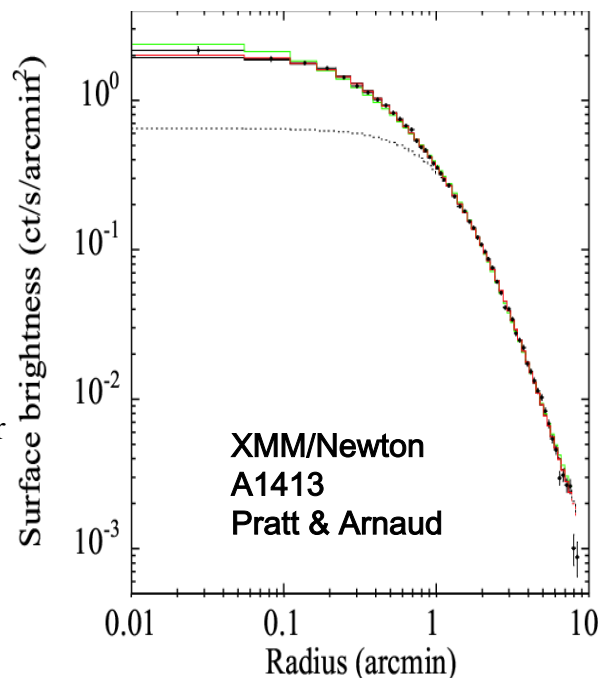
- It has become customary to use a ' β ' model (Cavaliere and Fesco-Fumiano)

- clusters have $\langle \beta \rangle \sim 2/3$

$$\rho(r) = \frac{\rho_0}{\left[1 + \left(\frac{r}{r_c}\right)^2\right]^{3\beta/2}}$$

$$\beta \equiv \frac{\mu m_p \sigma_{gal}^2}{kT} \text{ but treat as fitting parameter}$$

$$I_X(r) \propto \left[1 + \left(\frac{r}{r_c}\right)^2\right]^{-3\beta+1/2}$$



X-ray Mass Estimates

- use the equation of hydrostatic equilibrium

$$\frac{dP_{\text{gas}}}{dr} = \frac{-G\mathfrak{M}_*(r)\rho_{\text{gas}}}{r^2} \quad (3)$$

where P_{gas} is the gas pressure, ρ_{gas} is the density, G is the gravitational constant, and $\mathfrak{M}_*(r)$ is the mass of M87 interior to the radius r .

$$P_{\text{gas}} = \frac{\rho_{\text{gas}}KT_{\text{gas}}}{\mu\mathfrak{M}_H} \quad (4)$$

where μ is the mean molecular weight (taken to be 0.6), and \mathfrak{M}_H is the mass of hydrogen atom.

$$\frac{KT_{\text{gas}}}{\mu\mathfrak{M}_H} \left(\frac{d\rho_{\text{gas}}}{\rho_{\text{gas}}} + \frac{dT_{\text{gas}}}{T_{\text{gas}}} \right) = \frac{-G\mathfrak{M}_*(r)}{r^2} dr, \quad (5)$$

which may be rewritten as:

$$-\frac{KT_{\text{gas}}}{G\mu\mathfrak{M}_H} \left(\frac{d\log \rho_{\text{gas}}}{d\log r} + \frac{d\log T_{\text{gas}}}{d\log r} \right) r = \mathfrak{M}_*(r) \quad (6)$$

Putting numbers in gives

$$M(r) = -3.71 \times 10^{13} M_{\odot} T(r) r \left(\frac{d \log \rho_g}{d \log r} + \frac{d \log T}{d \log r} \right)$$

where T is in units of keV and r is in units of Mpc

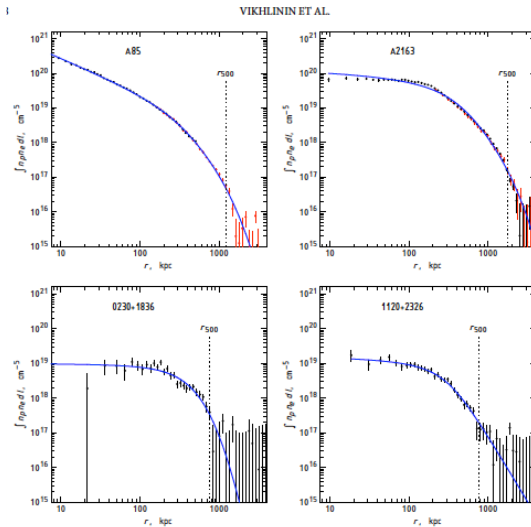


FIG. 5.— Examples of the surface brightness profile modeling for clusters shown in Fig. 3 and 4. The observed X-ray count rates are converted to the projected emission measure integral (see § 3.4 and Yee). The black and red data points show the Chandra and ROSAT measurements, respectively. The best fit model (the projected emission measure integral for the three-dimensional distribution given by eq. 2) is shown by solid lines. The dashed lines indicate the estimated r_{500} .

Hitomi to the Rescue

- Hitomi observations of the Perseus cluster measured both the mass motion and 'turbulence' of the gas (Hitomi Collaboration, 2016 Nature, 535, 117 and 2017a, arXiv:1711.00240)

- The width of a variety of lines is consistent with $\sigma=148\pm 6$ km/sec
- Energy content due to small scale motions (turbulence) ~4% and mass motion is even less

$$V_{\text{sound}} \sim 1000 \text{ km/sec } T_{4\text{keV}}^{1/2}$$

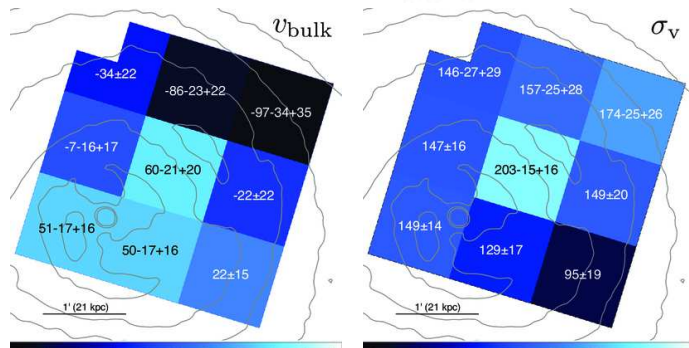
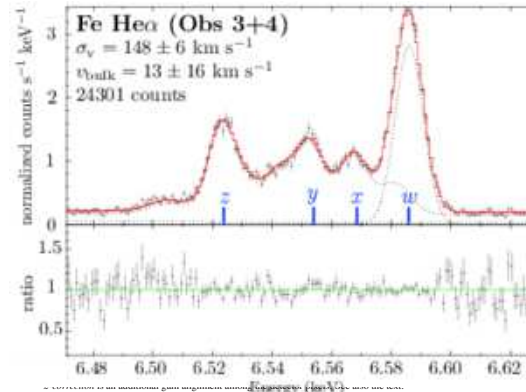
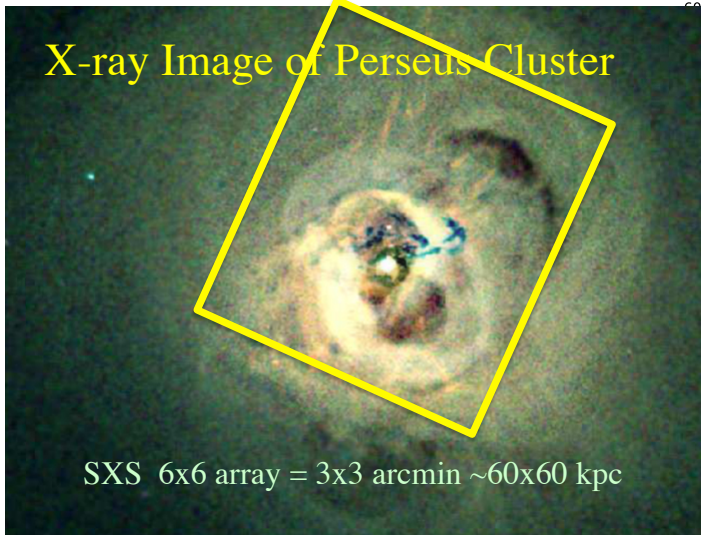
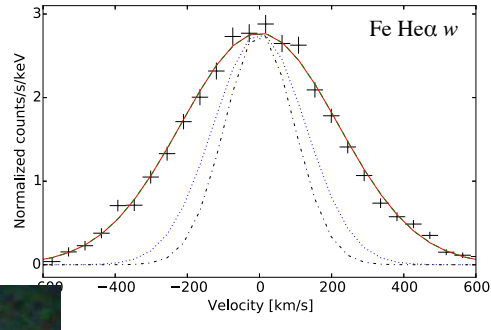


Fig. 4. Benchmark velocity maps. Left: bulk velocity (v_{bulk}) map with respect to $z = 0.017284$ (heliocentric correction of -26.4 km s^{-1} applied). Right: LOS velocity dispersion (σ_v) map. The unit of the values is km s^{-1} . Chandra X-ray contours are overlaid. The best-fitting value is overlaid on each region. Only Obs 3 is used and PSF correction is not applied.

Hitomi to the Rescue

- Indicating the reason for the “quiescent” nature of the plasma is the lack of strong drivers of gas motions in the core despite the presence of a strong AGN and x-ray structure

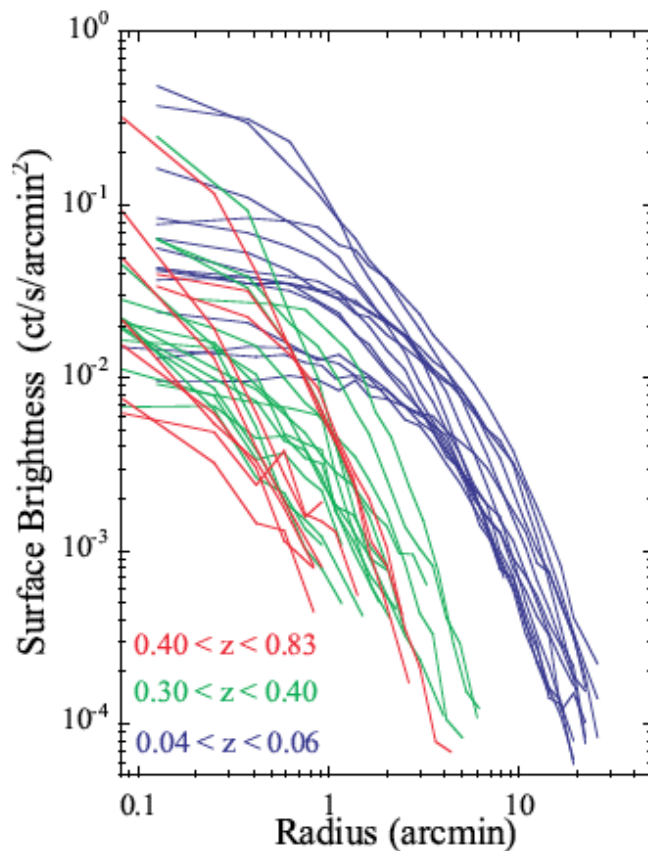


X-ray

Emissivity

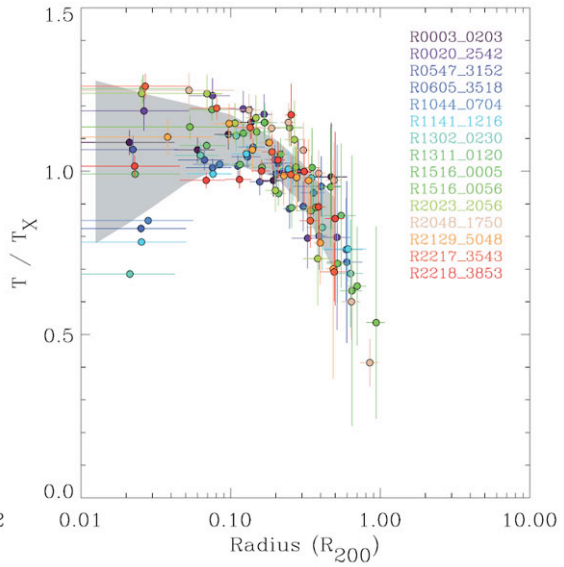
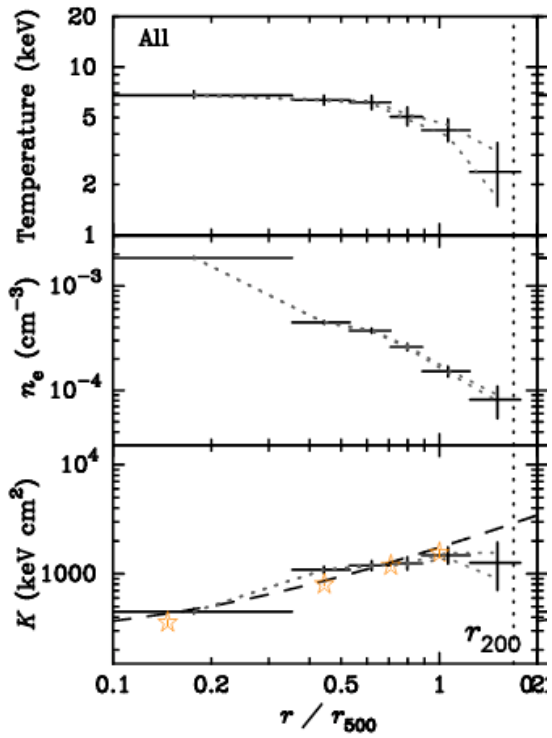
- The observed x-ray emissivity is a projection of the density profile

A large set of clusters over a wide range in redshift



X-ray Temperature Profiles

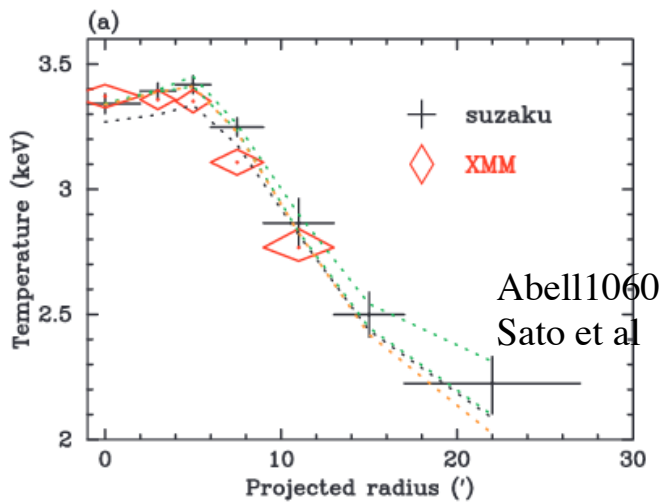
K. Sato et al



Pratt 2007

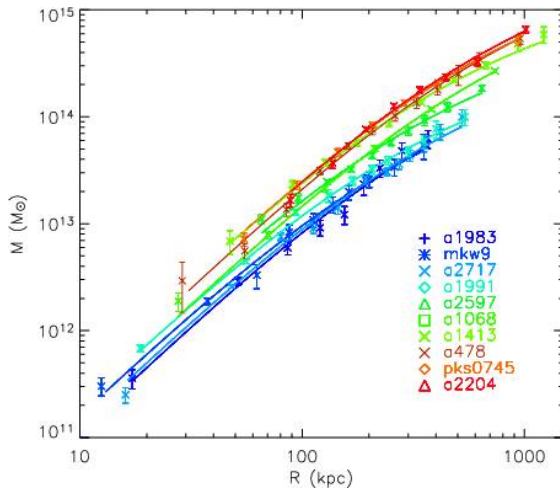
X-ray Temperature Profiles

- Comparison of two satellites

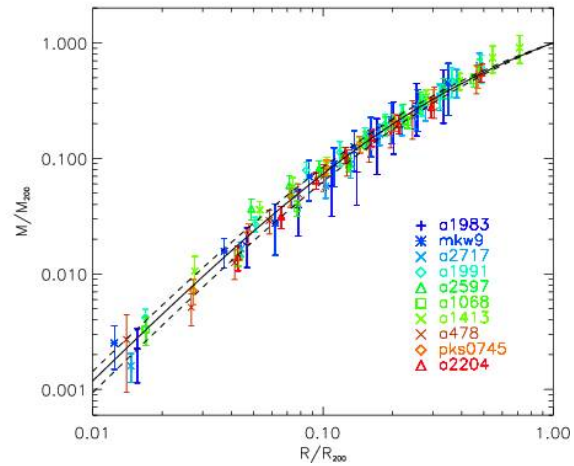


Mass Profiles from Use of Hydrostatic Equilibrium

- Use temperature and density profiles + hydrostatic equilibrium to determine masses



Physical units



Scaled units

- Scaled total density and gas density for a sample of clusters- yellow line is the NFW model
- Vikhlinin ApJ 640:691–709

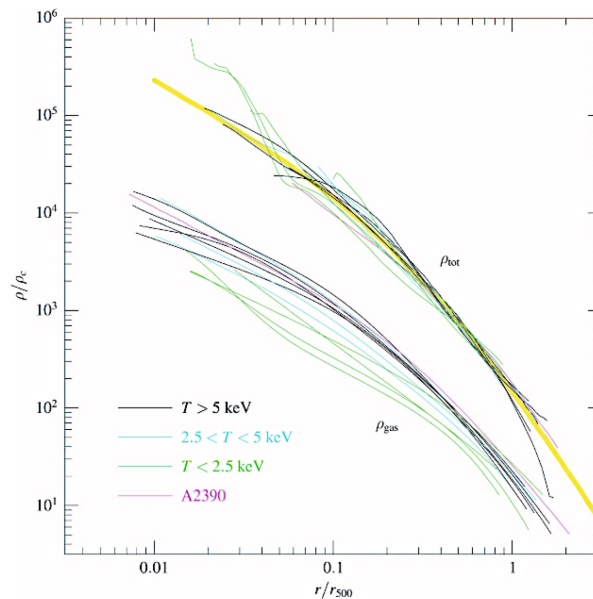
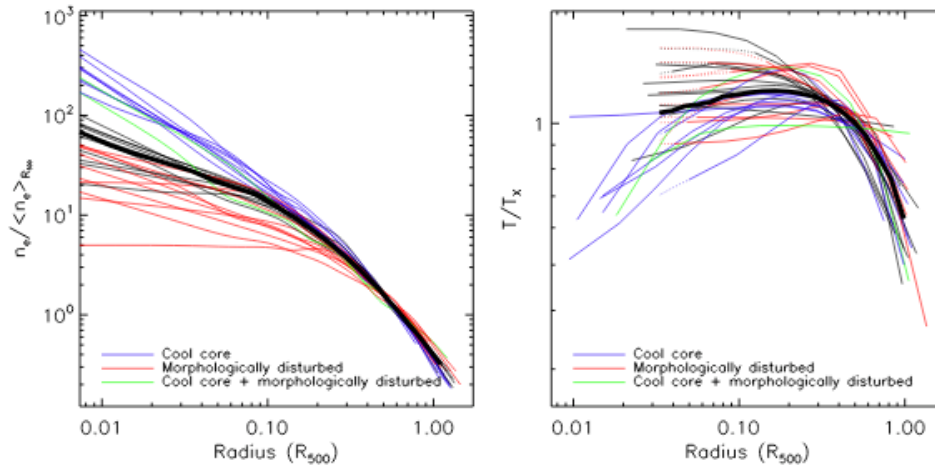


FIG. 17.— Scaled density profiles. Total density profiles are plotted within the radial range covered by the temperature profile. Gas density profiles are extended to r_{dec} (see Table 2). The thick yellow line shows the NFW model with $c_{500} = 3$, a typical value for CDM halos in our mass range (§ 6.1; see Fig. 18).



Arnaud et al 2010

Checking that X-ray Properties Trace Mass

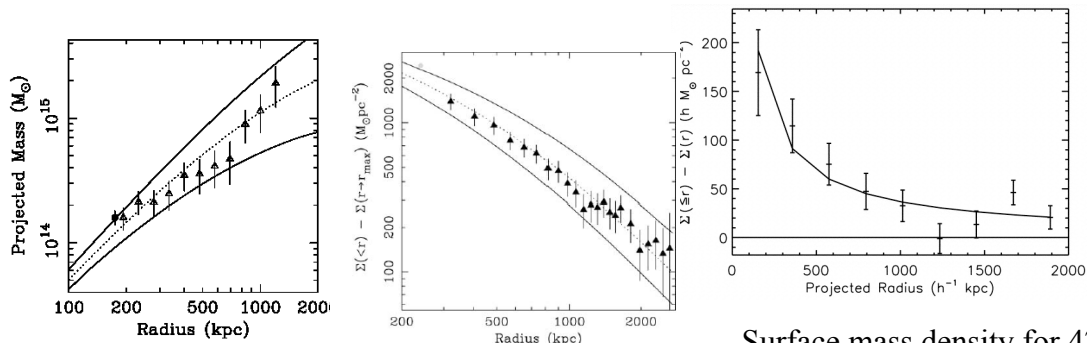


Figure 8. A comparison of the projected total mass determined from *Chandra* X-ray data (Section 5) with the strong lensing result of Pierre et al. (1996; filled circle) and the weak lensing results of Squires et al. (1999; open circle).

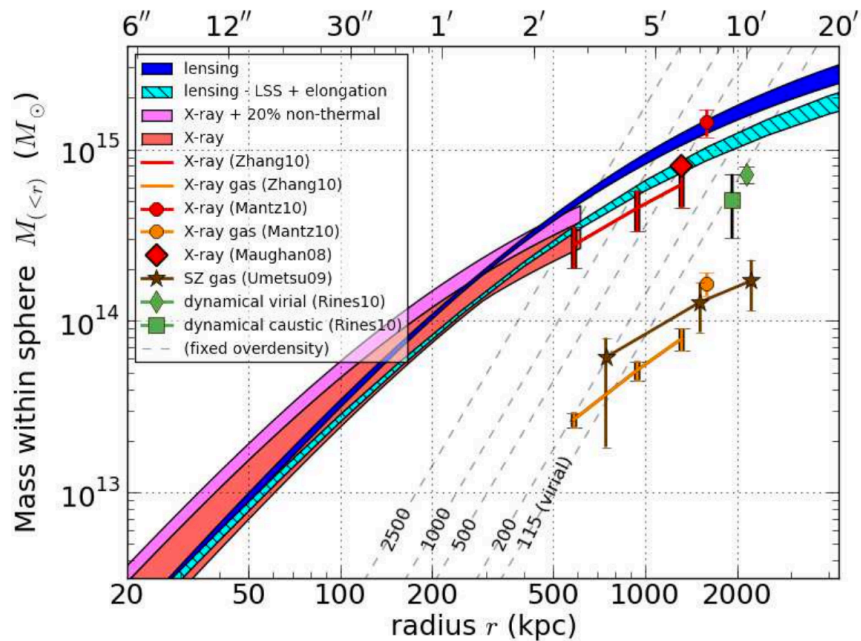
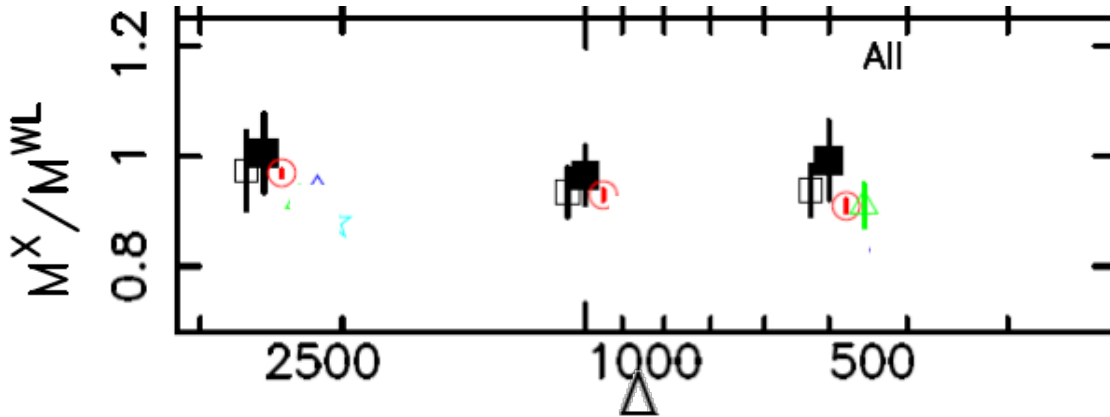
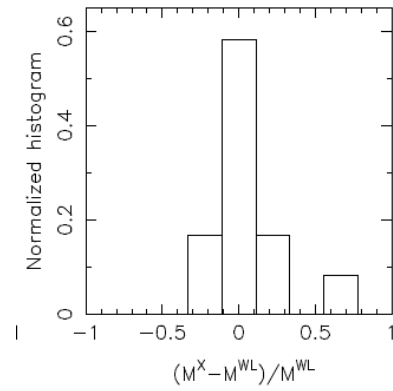
Surface mass density for 42 Rosat selected clusters from Sloan lensing analysis fitted with NFW profile

Comparison of cluster mass from lensing and x-ray hydrostatic equilibrium for A2390 and RXJ1340 (Allen et al 2001)

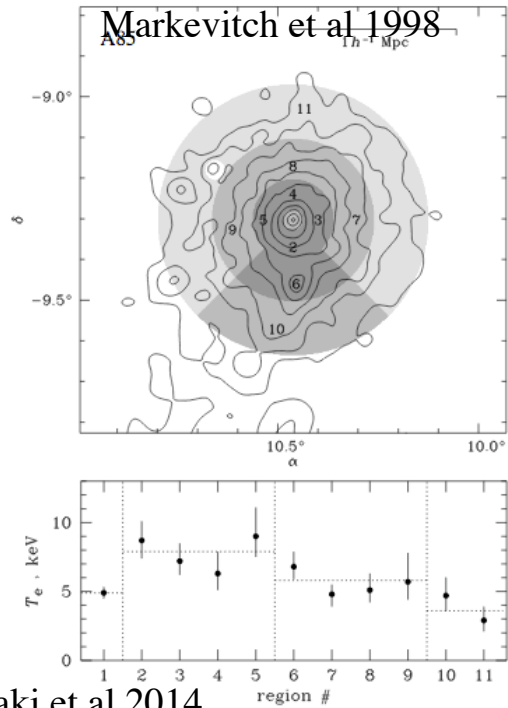
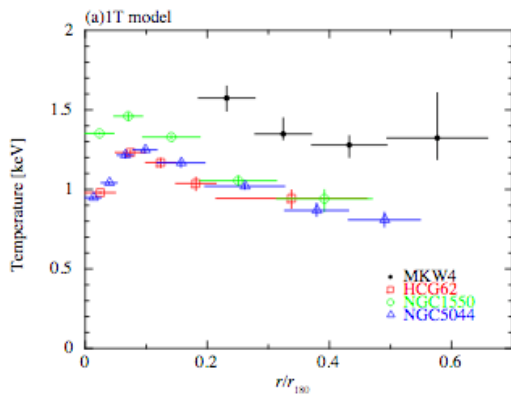
At the relative level of accuracy for smooth relaxed systems the x-ray and lensing mass estimators agree

Comparison of Lensing to X-ray Masses

- Δ is the overdensity of the part of the cluster used for the observations of the cluster mass compared to the critical density of the universe at the redshift of the cluster
- M_x is the mass from x-ray observations and assumption of hydrostatic equilibrium
- M_L is the mass from weak lensing



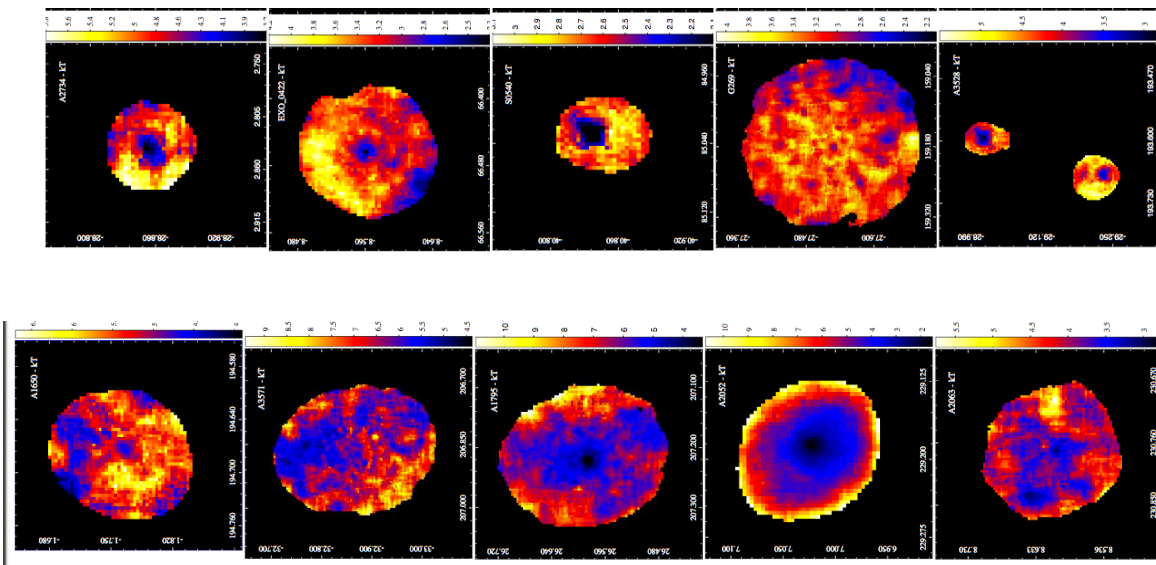
- Comparison of different observational techniques A2261
Coe et al. (2012)



4 low mass ($\sim 10^{14}M$) systems- Sasaki et al 2014

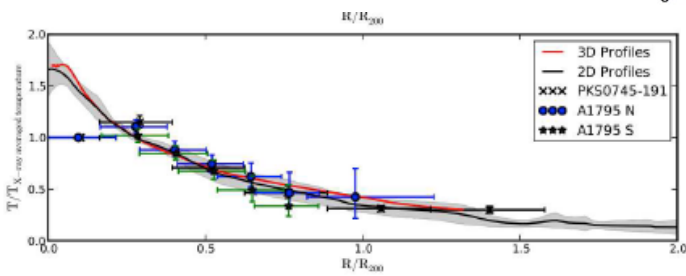
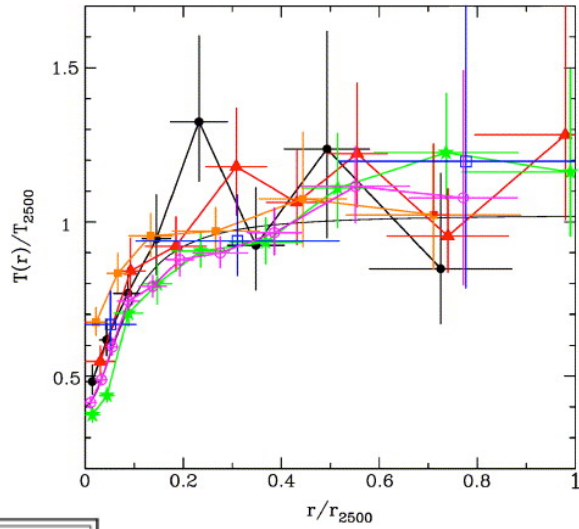
Cluster Temperature Structure

- 2-D cluster temperature maps Lagan'a, Durret & Lopes 1901.03851.pdf



Observed Temperature Profiles

- If the gas is in equilibrium with the potential (of the NFW form) it should be hotter in the center
- But in many clusters it is cooler in the center- additional physics



Left panel (from Burns et al 2010) shows the theoretical temperature profile if a NFW potential (in grey) compared to an set of actual cluster temperature profiles